QUANTITATIVE RISK ASSESSMENT (QRA) FOR NATURAL HAZARDS

Edited by Nasim Uddin, Ph.D., P.E. and Alfredo H.S. Ang, Ph.D.

ASCE Council on Disaster Risk Management
Monograph No. 5
June 2011

ASCE

QUANTITATIVE RISK ASSESSMENT (QRA) FOR NATURAL HAZARDS

EDITED BY
Nasim Uddin, Ph.D., P.E.
University of Alabama, Birmingham

Alfredo H. S. Ang, Ph.D.
University of California, Irvine

ASCE Council on Disaster Risk Management
Monograph No. 5

ASCE AMERICAN SOCIETY OF CIVIL ENGINEERS

Library of Congress Cataloging-in-Publication Data

Uddin, Nasim.
Quantitative risk assessment (QRA) for natural hazards / edited by Nasim Uddin, Alfredo H. S. Ang.
p. cm. – (Monograph / ASCE Council on Disaster Risk Management ; no. 5)
Includes bibliographical references and index.
ISBN 978-0-7844-1153-7
1. System safety--Mathematics. 2. Structural analysis (Engineering)--Approximation methods. 3. Natural disasters--Risk assessment. 4. Civil engineering--Decision making. 5. Quantitative research. I. Ang, Alfredo Hua-Sing, 1930- II. ASCE Council on Disaster Risk Management. III. Title. IV. Title: Quantitative risk assessment for natural hazards.

TA169.7.U33 2011
624.1'7--dc23 2011025245

American Society of Civil Engineers
1801 Alexander Bell Drive
Reston, Virginia, 20191-4400

www.pubs.asce.org

ISBN 978-0-7844-1153-7
Manufactured in the United States of America.

Council on Disaster Risk Management

Executive Committee (EXCOM)
Nasim Uddin, Ph.D., P.E., F.ASCE, Chair
Yumei Wang, P.E., F.ASCE, Vice Chair
James Beavers, Ph.D., P.E., F.ASCE Secretary
Vilas Mujumdar, Ph.D., P.E. Member
Anne Kiremidjian, Ph.D., M.ASCE, Past Chair

Advisory Committee
Alfredo H.S. Ang, Ph.D., Hon.M.ASCE
Amar Chakar, Ph.D., M.ASCE
Craig Taylor, Ph.D., Aff.M.ASCE
Erik VanMarcke, Ph.D., M.ASCE
Bilal M. Ayyub, Ph.D., PE, F.ASCE

Technical Committees & Chair
Mitigation Pre- & Post-Disaster
Chair: Steven Bartlett, Ph.D., PE, M.ASCE
Vulnerability & Risk
Chair: Bilal M. Ayyub, Ph.D., PE, F.ASCE
Outreach Education, Policy, Training & Programs
Chair: Berrin Tansel Ph.D., PE, D. WRE, F.ASCE

ASCE Staff
John Segna, Catherine Tehan

Activities & Products
Journal of Natural Hazards Review (NHR)
Monographs
Post Disaster Investigations
Conferences
Symposia
Join CDRM at *www.asce/taccdrm.com*

This page intentionally left blank

Contents

This page intentionally left blank

Introduction—Quantitative Risk Assessment (QRA) for Natural Hazards

This introduction and executive summary covers the origins of this monograph as a sequel to the five previous monographs generated by ASCE CDRM members and other volunteers as well as a brief synopses of the papers included in this monograph.

The Monograph as a Sequel

This monograph, produced by the Council on Disaster Risk management (CDRM), is a sequel to five previous monographs, *Acceptable Risk Processes: Lifelines and Natural Hazards* (2002) and ASCE CDRM Monograph No. 1, *Infrastructure Risk Management Processes: Natural, Accidental and Deliberate Hazards* (2006), both edited by Craig Taylor and Erik VanMarcke; *Disaster Risk Assessment and Mitigation* (2008) edited by Nasim Uddin and Alfredo Ang; *Multihazard Issues in the Central United States* (2008), edited by James Beavers; and *Windstorm and Strom Surge Mitigation* (2009) edited by Nasim Uddin.

Genesis of This Monograph

Recent events throughout the world have drawn attention to the vulnerability of infrastructure to natural hazards. Moreover, a risk analysis of any asset is not complete unless natural hazards are considered. Natural hazards include, at a minimum, the effects of earthquake, hurricane, tornado, and flood. Each of these events can be considered for any particular asset by determining the expected frequency of the event and estimating the consequences. The vulnerability of the asset is dependent upon the type of structure and how it will be affected by the initiating event. Additional natural hazards, such as ice storms, extreme cold weather, wildfire, avalanche, tsunami, landslide, mud slide, and others, should be included if the probability of occurrence and the consequences are higher than the four natural hazards mentioned above. This monograph is based on the ASCE tutorial and workshop organized by Prof. Alfredo Ang of the University of California at Irvine titled "Engineering Application of QRA" held during the fourth Civil Engineering Conference in the Asia region (4^{th} CECAR, June 25-27, Taipei, 2007). The QRA program included a morning session and an afternoon session.

In the morning session, Prof. Ang presented a tutorial titled "Introduction to Fundamentals for Quantitative Risk Assessment." The first paper of the monograph is based on the tutorial and titled "An Application of Quantitative Risk Assessment in Infrastructures Engineering," which summarized the practical aspect of quantitative risk assessment (QRA) highlighting engineering decision-making with emphasis on the design of civil infrastructures. Besides the estimation of the expected risk measure, the distribution of the risk resulting from the uncertainty in the calculated risk is equally important; the latter provides more complete information and permits the decision-maker the option of selecting a risk-averse measure to minimize the error (or increase the confidence) in making the right decision. Quantitative risk is also of significance for developing risk-based optimal design of infrastructures for mitigating risks from natural hazards. The process is illustrated numerically with a hypothetical example of the risk assessment (including risk reduction) and of retrofitting the levee system in New Orleans assuming that an assessment is performed in 1990—15 years prior to the occurrence of Katrina in 2005. The practical implementation of QRA is also emphasized.

The next six papers on the monograph are based on the six full papers presented in the afternoon session.

In the monograph's second paper titled *Quantitative Risk Analysis Applied to Dams*, Prof. Erik Vanmarcke explored the value and use of probabilistic risk assessment, with a focus on an action-oriented approach to decision-making applicable to (systems of) dams, in which the engineer estimates dam failure risks and their consequences and quantifies the effectiveness and economic benefits of alternative strategies aimed at risk reduction. The methodology presented in his paper provides a format for summarizing and accounting for (in the case of dams) data about past dam failures, the relative frequency of various causes of failure, the consequences of failure, and the effectiveness of different risk mitigation measures. It facilitates communication about risk and the costs and benefits of reducing risk among stakeholders in decision situations involving mitigation of hazards. Most importantly, it enables quantifying the benefits of actions aimed primarily at risk reduction. In this broad and varied context, the concepts and tools of quantitative risk analysis appear essential to advancing the art and practice of civil engineering.

In the third paper, *Risk Assessment for Wind Hazards*, Prof. Nasim Uddin discussed current wind-related quantitative risk assessment methodologies with examples. Recent research developments on modeling wind speed extremes associated with tropical cyclones and tornadoes are also briefly summarized in the paper.

Prof. Anne Kiremidjian, with co-authors Evangelos Stergiou and Renee Lee in their paper titled *Quantitative Earthquake Risk Assessment*, presented a brief summary of earthquake risk assessment methods. The method considers ground motion, liquefaction, and landslide hazards as well as the contribution of direct physical loss and functional loss, and can be applied either to a single structure or to group of structures that are spatially distributed in a region exposed to earthquakes. Furthermore, lifeline systems, such as water, power, communications, and transportation systems, can be analyzed with the consideration of the network flow through the system. For either a single structure or a distributed system, the risk can be due to direct damage or to loss of functionality. An example demonstrates the application of the method to a transportation network system within the San Francisco Bay Region.

In their paper *Risk Assessment for Bridge Decision-Making,* Prof. Dan M. Frangopol and Thomas B. Messervey investigate how the inclusion of risk can enhance the design, assessment, and management of bridge structures. The effect of obtaining more precise information is modeled through the reduction of the standard deviation of random variables within performance functions used to model a structure's performance over time within a reliability analysis. Similarities are investigated between the risk-based decision-making process and reliability-based life-cycle management (LCM) methods with the intent of combining synergistic benefits from each approach. A pre-posterior analysis in a Bayesian framework is conducted to demonstrate how life-cycle cost analysis can be utilized to facilitate the design of monitoring solutions by establishing cost/benefit benchmarks for consideration by bridge managers.

Prof. Bilal M. Ayyub and William L. Mcgill in their paper, *An All-Hazards Methodology for Critical Asset and Portfolio Risk Analysis,* develop a quantitative all-hazards methodology for critical asset and portfolio risk analysis (CAPRA) that considers both natural and human-caused hazards. The data requirements for CAPRA include both historical information and expert opinions, and uncertainty is accommodated as appropriate using standard techniques for uncertainty propagation and representation. A general formula for all-hazards risk analysis is obtained that resembles the traditional model based on the notional product of consequence, vulnerability, and threat, though with clear meanings assigned to each parameter. The methodology is briefly introduced and demonstrated using several illustrative examples based on notional information.

In the final paper of the monograph, *A Methodology for the Risk Analysis and Management of Protected Hurricane-Prone Regions*, Prof. Ayyub introduces a quantitative risk analysis methodology for hurricane prone areas protected by a hurricane protection system. The methodology is intended to assist decision-makers and policy-makers, and has the characteristics of being analytic, quantitative, and probabilistic. Quantifying risk using a probabilistic framework produces hazard (elevation) and loss-exceedance rates based on a spectrum of hurricanes according the joint probability distribution of the characteristic parameters that define hurricane intensity and the resulting surges, waves, and precipitation. The hazard is quantified using a probabilistic framework to obtain hazard profiles as elevation-exceedance rates, and the risk is quantified in the form of loss-exceedance rates based on a spectrum of hurricanes determined using a joint probability distribution of the parameters that define hurricane intensity. The proposed methodology will enable decision-makers to evaluate alternatives for managing risk, such as providing increased hurricane protection, increasing evacuation effectiveness, changing land use policy, enhancing hurricane protection system operations, and enhancing preparedness.

In conclusion, the monograph should appeal to all those concerned with safeguarding infrastructures from the effects of natural hazards. With its team of expert contributors, who reflect many years of specialized experience, including the private, governmental, and academic perspectives, the monograph will be a standard reference in many fields of engineering including risk assessment, disaster management, engineering mechanics, and structural engineering. It can serve as the reference text of risk assessment for disaster management course on homeland security.

Chapter 1: An Application of Quantitative Risk Assessment in Infrastructures Engineering

By A. H-S. Ang, University of California, Irvine

Abstract

The practical aspect of quantitative risk assessment (QRA) is highlighted for engineering decision-making with emphasis on the design of civil infrastructures. Besides the estimation of the expected risk measure, the distribution of the risk resulting from the uncertainty in the calculated risk is equally important; the latter (the distribution) provides more complete information and permits the decision-maker the option of selecting a risk-averse measure to minimize the error (or increase the confidence) in making the right decision. Quantitative risk is also of significance for developing risk-based optimal design of infrastructures for mitigating risks from natural hazards. The process is illustrated numerically with a hypothetical example of the risk assessment (including risk reduction) and of retrofitting the levee system in New Orleans assuming that an assessment is performed in 1990, 15 years prior to the occurrence of Katrina in 2005. The practical implementation of QRA is emphasized.

Introduction

Engineers deal with risks all the time; however, these risks are seldom in quantitative terms. They are generally in qualitative terms and are dealt with intuitively based on engineering judgments. For example, major designs are performed through the use of *factors of safety*. Such factors are required to cover uncertainties inherent in materials, in the specified loadings, and in the calculational models, and are intended to minimize the risk underlying a design. The use of such safety factors is proper and serves to greatly simplify the design process; however, the proper values of these factors ought to be consistent with an acceptable or tolerable risk underlying a design. For this latter purpose, quantitative evaluations of the risk and of its uncertainty are relevant and are needed in order to make the proper risk-informed decisions in the determination of the appropriate factors of safety.

In the case of natural hazards, risk is most meaningful when expressed in terms of potential human sufferings and/or economic losses. Besides the probability of occurrence of a hazard, risk must include the potential adverse consequences that can result from the hazard event. The risk associated with natural hazards are very real, such as from strong earthquakes and associated tsunamis, high hurricanes (or typhoons), tornadoes, floods, and massive landslides. The forces created or induced by such natural hazards are usually extremely high and can cause severe damages and failures of engineered systems. Engineers, however, must still plan and design such structures and infrastructures in spite of the extreme forces produced by one or more of these natural hazards. How safe should these infrastructures or facilities be for resisting the forces of natural hazards, of course, depends on the capital investments that stakeholders, such as a government entity responsible for funding, are willing to make (for safety and reliability) to prepare and protect against or reduce any impending risk to future hazards. To make the proper decisions on needed or optimal investments, information on risk and associated risk reduction accruable from additional investment are clearly pertinent; this technical information must be provided to the decision-makers.

In formulating engineering decisions, such as for the design of infrastructures against the forces of natural hazards, the significance of calculated risks in terms of potential damage and other adverse consequences cannot be over-emphasized. However, the uncertainty (of epistemic type) in a calculated risk is equally significant and relevant. In this regard, it is the engineer's primary responsibility to provide the proper technical information to the decision-makers and stakeholders in the construction of protective infrastructure systems for mitigating a hazard. For this latter purpose, quantitative risk assessment methodology provides the tools needed. The fundamentals of QRA are summarized below with an example illustrating the numerical process of assessing risk for natural hazard mitigation and of estimating related risk reduction. The same example also illustrates the application of QRA in formulating optimal design based on whole life cost consideration. Although the application to infrastructures for natural hazard mitigation is emphasized and illustrated, the same QRA concepts apply equally to other applications in civil engineering.

Quantitative Risk-Assessment Methodology

Information on risk is often presented in qualitative terms, for example, as high, medium, or low. More often than not, information in this form is ambiguous and difficult to interpret; moreover, it is not possible to perform risk-benefit trade off analysis, which is often needed for formulating optimal decisions. For this latter purpose, risk needs to be expressed in quantitative terms, such as potential number of fatalities and injuries, and/or potential economic losses in the case of natural hazards. Similarly, quantitative risk information is needed to assess the benefit of investment in risk reduction from which the benefit associated with a reduction in risk can be made transparent and meaningful and provide the basis for a proper benefit-risk study. QRA is relevant also in the development of optimal designs for minimum life-cycle cost.

Uncertainty in Estimated Risk

In assessing risk, especially relative to natural hazards, significant uncertainties can be expected. The occurrence of a given hazard within a given time window, such as a strong-motion earthquake in a particular region of the world, is unpredictable; moreover, the damaging effects of the earthquake are highly variable and difficult to estimate with precision. Also, the human casualties and sufferings as well as the financial and economic losses that are possible consequences following the earthquake are often difficult to quantify and, therefore, may only be assessed judgmentally. It is, thus, easy to recognize that there is considerable uncertainty in the quantitative assessment of risk associated with natural hazards or similar extreme events. Such uncertainties, however, are important and the evaluation of their significance is the essence of a quantitative risk assessment.

Uncertainties may be classified into two broad types (see e.g., Ang and Tang, 2007)—namely, the aleatory and the epistemic types. The aleatory type is data-based and is associated with the natural randomness or inherent variability of a phenomenon; whereas, the epistemic type is knowledge-based due to our insufficient knowledge for predicting the phenomenon and in estimating the associated effects and consequences. In this regard, the aleatory uncertainty would give rise to a calculated risk, whereas the epistemic uncertainty would define the range or distribution of possible risk measures (representing the uncertainty in the calculated risk). Both the calculated risk and its uncertainty are equally important. It is, therefore, important to clearly differentiate the two types of uncertainty and properly delineate their respective effects. Irrespective of the type of uncertainty, however, the basic tools for its modeling and the analysis of the respective effects require the same principles of probability and statistics.

Probability Models in QRA

Probability models, therefore, are the basic tools for quantitative risk assessment. However, risk is more than just probability; it must include the potential consequences from the occurrence of an adverse event. In the case of natural hazards, the occurrence of a particular hazard in time and location is invariably unpredictable, and its destructive effects on structures and infrastructures are highly variable. Finally, the resulting consequences of the destructive effects invariably contain significant uncertainty. Therefore, for quantitative considerations, each of these aspects may be modeled and evaluated using probability models as outlined below (see also Ang 2006a).

QRA will generally consist of three components, which may be defined, respectively, as follows:

1. *hazard analysis*—the determination of the probability of occurrence of an adverse event within a given time window;
2. *vulnerability analysis*—the estimation of the extent and severity of damage to made-made and protective systems, and
3. *consequence analysis*—the estimation of the potential consequences caused by the occurrence of the adverse event.

The product of the above three components constitutes the estimated risk, R; that is

$$R = H_z \times V_u \times C_q \tag{1-1}$$

where: H_z = the result of a probabilistic hazard analysis;
V_u = the result of a vulnerability analysis; may be in terms of the probability or fraction of damage to existing infrastructures;
C_q= the estimated potential consequences resulting from the occurrence of the adverse event.

As there are epistemic uncertainties in estimating or calculating each of the components in Eq. 1-1, the calculated risk will also contain uncertainty leading to a range (or distribution) of the possible risk measures. It might be pointed out that the aleatory and epistemic uncertainties may be combined into a total uncertainty; in such a case, however, the resulting calculated risk will represent only the mean (or "best estimate") value of R.

Analysis of Hazard or Adverse Event

The determination of the occurrence probability of an adverse event, such as a natural hazard, will obviously depend on the particular hazard. For example, in the case of earthquake hazards, probabilistic models for seismic hazard analysis are well established (e.g., Cornell 1968; Der Kiureghian and Ang 1977); such models and associated recent refinements (e.g., Harmsen 2005) are now widely employed in practice. Similarly, models for the hazard analysis of tornado strikes have been developed by Wen and Chu (1973); whereas, for wind storms and hurricanes and riverine floods, the respective occurrence probabilities at a given location over a specified period may be estimated from appropriate local or regional statistical data, modeled by extreme-value distributions (e.g., Gumbel 1954) as appropriate.

Vulnerability Analysis

Given the occurrence of a particular hazard, there is some chance that facilities or infrastructures within the affected zone will be severely damaged or collapsed. This probability, of course, will depend on the distribution of the maximum force from the hazard relative to the capacities of the existing infrastructure systems for resisting such forces. As the maximum forces and the capacities will both contain variability and uncertainty, each may be represented with a probability model. That is, the maximum forces and capacities can be represented with respective random variables and associated probability distributions. A vulnerability analysis may then be performed and should yield the fraction of damage or failure to existing infrastructure systems in a city or regional area

Analysis of Consequences

The adverse consequences caused by an extreme event may be very severe, such as large magnitude earthquakes, high category hurricanes (or typhoons), or massive landslides and mudflows. These may often involve large numbers of fatalities and injuries, high economic and financial losses, major disruptions of utilities and transportation facilities, and related indirect consequences caused by ripple effects. The estimation of the consequences associated with the occurrence of a given event is often difficult and may have to be based largely on judgments, that is, relying on judgments from experts with knowledge gained through experience from similar events. Even then, the estimated consequences would contain significant uncertainties (of epistemic type) and may be expressed only as respective ranges of possible losses.

Role of QRA in Optimal Design of Infrastructure Systems

Optimal design of engineering facilities or infrastructures may be based on minimizing the expected life-cycle cost, E(*LCC*). On this basis, the same optimal design would be obtained when other percentile values of the *LCC* are used in the optimization process; this has been verified by Ang and De Leon (2005). However, for risk-informed decisions, higher percentile values (such as the 75 percent or 90 percent value) rather than the mean or median value, of the *LCC* may be selected or specified in order to minimize the chance of under estimating the actual life-cycle cost for the optimal design (Ang 2006b).

A Numerical Illustration

An (hypothetical) example is described numerically below to illustrate the conceptual process of QRA as outlined above. In order to clarify the steps in the QRA process, the problem is necessarily idealized, although the assumptions are reasonably realistic. For this purpose, suppose that an analysis of the hurricane risk for New Orleans (for a period of 20 years) was performed 15 years (say in 1990) before the occurrence of Katrina, a Category 4 hurricane, in August 2005. In this illustrative example, the numerical values used are hypothetical and may not be completely accurate (as they are pre-Katrina). Nevertheless, they serve to illustrate the quantitative process of assessing the underlying risks and associated uncertainties[1] for the purpose of providing the essential quantitative information for making risk-informed decisions for mitigating a future hazard.

Assume that upon careful examination of the recorded data on hurricanes in the Gulf Coast region of the United States, the return period of a Category 4 hurricane striking the vicinity of New Orleans is determined to be around 100 years; this means that there is a 1 percent average probability each year, and approximately a 20 percent probability over a 20-year period, that a Category 4 hurricane can be expected to hit the city of New Orleans and its vicinity. A 20 percent probability of occurrence over a period of 20 years (which is not particularly long) is a significant probability.

A Category 4 hurricane, with a maximum sustained wind speed of 200-233 kph (125-145 mph) is bound to cause massive damages to ordinary dwellings and severe damages to some of the engineered infrastructures. Also, as the elevation of the city of New Orleans is 1.8 to 2.1 m (6 to 7 ft.) below sea level, the city is protected by the levees and floodwalls that kept the water of the surrounding lakes (such as Pontchartrain) and the Mississippi River from inundating the city. It has been widely reported that the levees were designed and constructed with an average height of around 2.44 m (8 ft.) for protection against hurricanes of Category 2 or 3. Suppose that the actual levee height varies with a symmetric triangular distribution between 7 and 9 ft. (2.1 and 2.7 m) and that the surges from the lake caused by a Category 4

[1] All the calculations in the example were performed through Monte Carlo simulations using MATLAB software with the accompanying Statistics Toolbox.

hurricane can be modeled with a lognormal random variable with an estimated median height of 10 ft. (3.1 m) and a c.o.v. of 30 percent. Therefore, under a Category 4 hurricane there is a high probability that the levees will be breached causing massive inundation of the city; with these assumptions, this probability can be calculated to be as follows: P(levee breached) = 0.78

Furthermore, the vulnerability of much of the houses in New Orleans and vicinity against the hurricane winds would also be very high. Assume that the distribution of sustained wind speed in a Category 4 hurricane is modeled with a Type I extreme-value distribution with a mean speed of 209 kph (130 mph) and a c.o.v. of 40 percent and that the wind speed resistance of houses and other structures is a lognormal random variable with a median of 85 mph (137 kph) and a c.o.v. of 30 percent. On these bases, the vulnerability of the building stock and other facilities in the city to the hurricane winds would be extremely high, as follows: Vulnerability of structures = 0.785

The consequences of the destructive effects of a Category 4 hurricane to the city of New Orleans, therefore, must include those caused directly by the high winds as well as by the surges from the lakes. Assuming that up to 90 percent of the population (approximately 600,000) in New Orleans will be evacuated before the storm, the potential fatalities may be assumed to range from 1,800 to 3,000 (that is, 3 percent to 5 percent of those who did not evacuate) and serious injuries between 5,000 and 10,000, with respective mean values of 2,400 fatalities and 7,500 injuries; whereas, the economic loss could range between $75 billion and $150 billion with a mean loss of $112.5 billion. It may be reasonable to assume (prior to the occurrence of Katrina) that the fatalities and injuries will be caused equally by the extreme wind and by the inundation of the city; whereas, the economic loss will largely be caused by the failure of the levee system and subsequent inundation of the city. These losses would largely be judgmental estimates (based on past experience with similar disasters when available).

On the basis of the above postulated information, the best estimate of the risks to the city of New Orleans can be summarized as follows (based on respective mean values):

Fatality risk = 0.5[0.20(0.785)(2400)] +
    0.5[0.20(0.78)(2400)] = 376

Risk of serious injuries = 0.5[0.20(0.785)(7500)]
    + 0.5[0.20(0.78)(7500)] = 1,174

Risk of economic loss (in dollars) =
    0.20(0.78)(112.5) = $17.55 billion

On Risk Reduction

The results of a quantitative risk assessment will permit also a quantitative analysis of the reductions in the respective risks that can accrue from an investment in strategies to mitigate the effects of a future hazard. A clear example would be the risk reductions accruing from strengthening and raising the height of the levees around New Orleans for protection against a Category 4 hurricane. Suppose that (in 1990) the cost to improve the levee system is estimated to be \$1 billion to ensure against or mitigate any inundation of the city. This may require raising the height from the existing average height of 2.44 m (8 ft.) to a uniform height of 3.66 m (12 ft.) plus any needed strengthening of the levees and floodwalls. With 3.66-m (12-ft.) levees, the probability of breaching from a Category 4 hurricane will be reduced to the following: P(levee breached) = 0.27; and the respective best estimate reduced risks would be as follows:

$$\text{Reduced economic risk} = 0.20(0.27)(112.5) = \$6.08 \text{ billion}$$

$$\text{Reduced fatality risk} = 0.5[0.20(0.27)(2400)] + 0.5[0.20(0.785)(2400)] = 253$$

$$\text{Reduced injury risk} = 0.5[0.20(0.27)(7500)] + 0.5[0.20(0.785)(7500)] = 791$$

Therefore, with the investment of \$1.0 billion to improve the levee system, the best estimate net reductions in the respective risks would be as follows:

$$\text{Reduction in economic risk} = (17.55 - 6.08 - 1.00) = \$10.47 \text{ billion;}$$

$$\text{Reduction in fatality risk} = (376 - 253) = 123\text{; and}$$

$$\text{Reduction in injury risk} = (1174 - 791) = 383,$$

which are significant reductions in the respective risks accruable from the \$1.0 billion investment for improving the levee system.

Distributions of Estimated Risks

The risks calculated above are based on the estimated mean (or median) values of the respective components in Eq. 1-1, yielding the best-estimate risk measures. Clearly, there are (epistemic) uncertainties in each of the estimated mean (or median) values in Eq. 1-1; these uncertainties may be represented by realistic ranges (or distributions) of the respective estimated mean (or median) values. These will lead also to corresponding distributions of the estimated risk measures, which are equally as important as the calculated mean risks. In the present example, these epistemic uncertainties would include specifically the following:

1. The estimated return period of 100 years for a Category 4 hurricane occurring in New Orleans may actually be between 50 to 150 years. In such a case, the annual occurrence probability would range between 0.7 percent and 2 percent (in 20 years would be 14 percent to 40 percent); the underlying uncertainty may then be represented by a c.o.v. of 29 percent, and may be modeled with a lognormal distribution with a median of 1.0 and a c.o.v. (coefficient of variation) of 0.29, i.e. LN(1.0, 0.29).

2. Because the specified estimated median surge height of 3.05 m (10 ft.) in the surrounding lakes may not be accurate, the actual median surge could vary between 2.44 and 3.66 m (8 ft. and 12 ft.). This is equivalent to a c.o.v. of 12 percent in the median surge height, which may be represented by a lognormal distribution of LN(1.0, 0.12). Therefore, the probability of breaching the levees would become a random variable and can be described by the histogram shown in Figure 1.1, which has a mean value of 0.75.

3. The mean wind speed of 130 mph (209 kph) in a Category 4 hurricane may actually be between 110 and 150 mph (177 and 241 kph). This is equivalent to a c.o.v. of 9 percent in the estimated mean wind speed. In this light, the vulnerability of structures and facilities in the region would also be a random variable.

4. Finally, the uncertainties in the estimated consequences (as indicated earlier) may be postulated as follows:
   - the economic loss ranging from $75 billion to $150 billion, assumed to be uniformly distributed within the indicated range;
   - the fatalities ranging from 1,800 to 3,000, assumed to be uniformly distributed within this range; and
   - the injuries ranging from 5,000 to 10,000, also assumed to be uniformly distributed within this range.

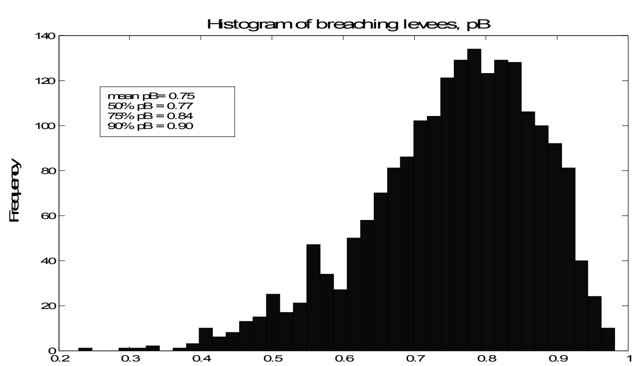

Fig. 1.1. Histogram of Probability of Breaching Levees, pB

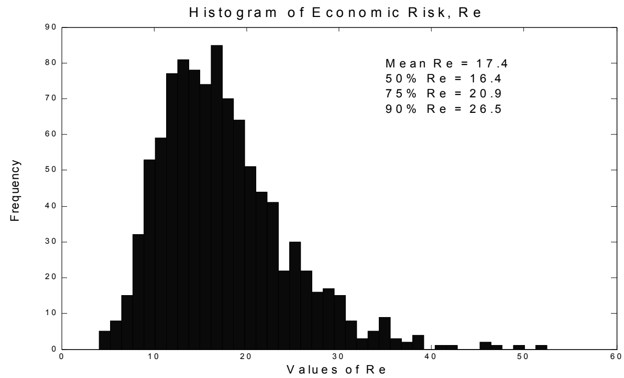

Fig. 1.2. Histogram of Economic Risk, Re

To take account of the above uncertainties, the resulting economic risk can be evaluated as

$$Re = 0.20NH(pB)(CE) \tag{1-2}$$

Eq. 1-2 is actually a convolution integral, in which

p_B = probability of breaching the levees; the histogram of Figure 1.1 contains the uncertainty in the estimation of the median surge height;

N_H = uncertainty in the estimated mean hazard (i.e., return period), prescribed as LN(1.0, 0.29);

C_E = economic loss from inundation of city, assumed to be uniformly distributed between \$75 and \$150 billion.

In light of the above uncertainties, the economic risk, Re, of Eq. 1-2 would also be a random variable. By Monte Carlo simulation (with 1,000 repetitions), we generate the corresponding histogram as shown in Figure 1.2 with a mean value of \$17.4 billion.

Of particular interest for decision making are the following percentile values of Re:

50 percent value = \$16.4 billion;
75 percent value = \$20.9 billion;
90 percent value = \$26.5 billion.

For example for a risk averse (conservative) decision, the 90 percent value may be selected or used; in which case, the economic risk from inundation caused by a Category 4 hurricane would be specified as \$26.5 billion instead of the best estimate value (or mean value) of \$17.5 billion. This 90 percent value would imply a possible error of 10 percent in contrast to an approximately 50 percent error in the best estimate value of the economic risk.

Similarly, because of the uncertainty in the estimated mean wind speed as well as in the occurrence probability of a Category 4 hurricane and in the expected number of fatalities, the fatality risk is also a random variable with the histogram shown in Figure 1.3 with a mean value of 385 fatalities.

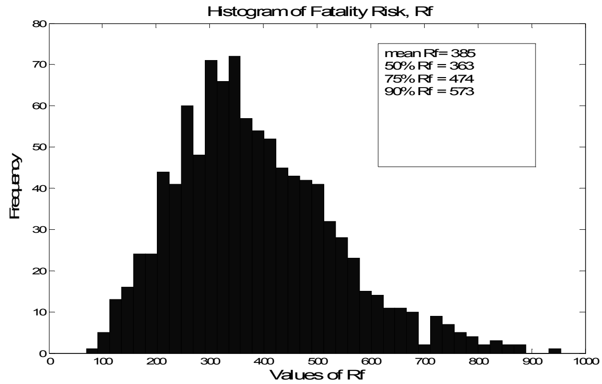

Fig. 1.3. Histogram of Fatality Risk, Rf

The following percentile fatality risk values may be of special interest for decision-making.

50 percent Rf = 363;
75 percent Rf = 474;
90 percent Rf = 593

For a risk averse (or conservative) decision, the 90 percent value of 593 fatalities may be specified.

Similarly, the distribution of the injury risk is shown in Figure 1.4 with a mean of 1,203 injuries. Again, the following percentile values of the injury risk would be of special interest in decision-making:

50 percent Rj = 1,135;
75 percent Rj = 1,477;
90 percent Rj = 1,864

in which the 90 percent value of 1,864 injuries would be a conservative risk value.

Finally, it is important to emphasize that by specifying a conservative or risk-averse value (such as the 90 percent value), the effects of uncertainty (of the epistemic type) in the calculated risk is reduced or can be minimized.

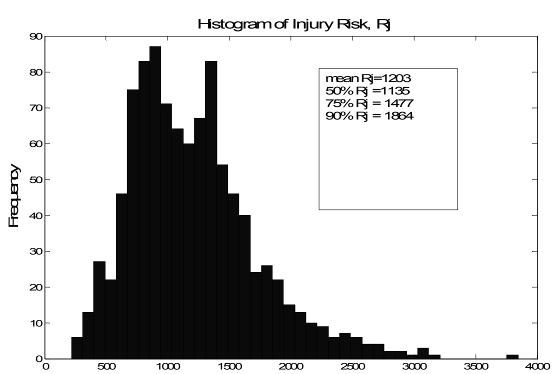

Fig. 1.4. Histogram of Injury Risk, Rj

Optimal Design Height of Levee System

Clearly, New Orleans will need a reliable levee system for retaining the water from the surrounding lakes and the Mississippi River as well as for protection of the city against serious flooding caused by future hurricanes. The cost to improve or retrofit the levee system will depend largely on the design height of the levees. Inversely of course, the economic risk will decrease with the levee height.

Suppose that the projected cost for improving the levee system will vary with the design height of the levees as shown in the first two columns of Table 1.1 below.

Table 1.1: Risk and E(*LCC*) for Different Levee Heights

Height of Levee, ft. (m)	Cost of Levee, US$billion	P(breaching)	E(Econ. Risk)	E(*LCC*), $billion
8 (2.44)	0.10	0.78	$17.60 billion	17.7
9 (2.75)	0.25	0.64	$14.40 billion	14.65
10 (3.05)	0.40	0.52	$11.70 billion	12.10
11 (3.36)	0.60	0.38	$8.55 billion	9.15
12 (3.66)	1.00	0.28	$6.30 billion	7.30
13 (3.97)	2.75	0.21	$4.73 billion	7.48
14 (4.27)	5.00	0.12	$2.70 billion	7.70
15 (4.58)	6.50	0.09	$2.03 billion	8.53

Suppose that (in 1990) the levee system was to be retrofitted to protect against future Category 4 hurricanes. Then over a 20-year period, the expected probabilities of breaching for the respective levee heights are shown in the third column of Table 1.1, and the corresponding expected economic risks are given in Column 4. The respective expected life-cycle costs, E(*LCC*), are therefore the costs of the levee system plus the expected economic risks (that is, Column 2 + Column 4), which are those shown in Column 5 of Table 1.1. Plotting the E(*LCC*) against the respective levee heights yields the graphic results shown in Figure 1.5.

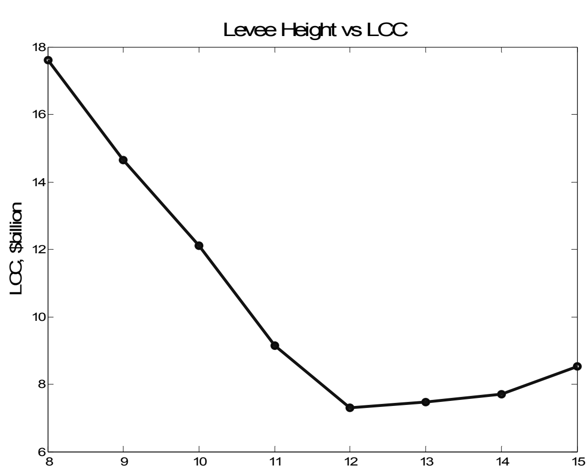

Fig. 1.5. E(LCC) vs Levee Height

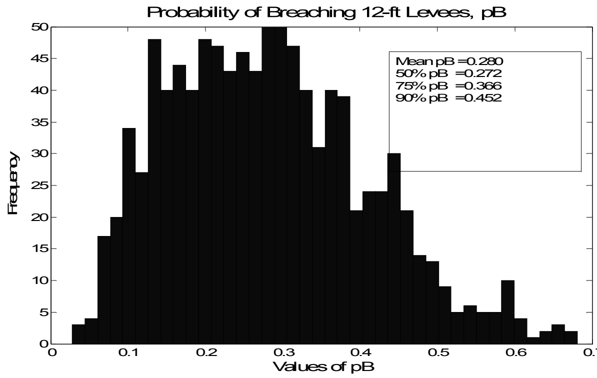

Fig. 1.6. Histogram of 20-year probability of breaching 12 ft. levees, pB

From Figure 1.5, it can be observed that the design height with the minimum E(*LCC*) would be 3.66 m (12 ft.) with an E(*LCC*) of \$7.30 billion. However, there are (epistemic) uncertainties in this estimated expected *LCC*; in particular, several underlying epistemic uncertainties would lead to the uncertainty (and thus a distribution) in the estimated *LCC*; these uncertainties would include specifically those that were identified earlier in assessing the respective risks. Specifically, because the estimated median surge height of 10 ft. in the surrounding lakes is uncertain, the actual median surge could vary between 2.44 m and 3.66 m (8 ft. and 12 ft.). The resulting probability of breaching the 12 ft. levees in 20 years would also become a random variable with the distribution (histogram) shown in Figure 1.6 which has a mean value of 0.280, and the following percentile values:

50 percent pB = 0.272
75 percent pB = 0.366
90 percent pB = 0.452

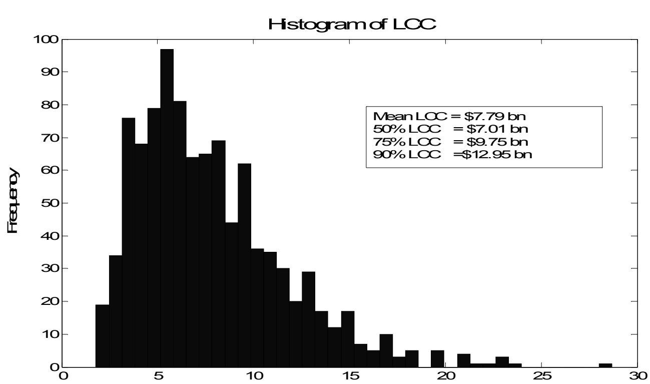

Fig. 1.7. Histogram of Life-Cycle Cost, LCC

Finally, to take account of the epistemic uncertainties enumerated earlier, the resulting *LCC* can be evaluated as

$$LCC = CI + 0.20NH(pB)(CE) \qquad (1\text{-}3)$$

in which the second term on the right hand side is a convolution integral, where

C_I = the initial cost of re-constructing or retrofitting the levee system;

p_B = probability of breaching the levees; histogram of Figure 1.6 contains the uncertainty in the estimation of the median surge height;

N_H = uncertainty in the estimated mean hazard (i.e., return period), prescribed as LN(1.0, 0.29);

C_E = economic loss from inundation of city assumed to be uniformly distributed between \$75 billion and \$150 billion.

In light of the above uncertainties, the *LCC* would also be a random variable. By Monte Carlo simulation (with 1,000 repetitions), we generate the corresponding histogram as shown in Figure 1.7 with a mean value of \$7.79 billion.

Safety Index for Structural Design of Levees

Finally, we observe from Figure 1.6 that the median probability of breaching the 12-ft. levee is 0.28 in 20 years, or an annual probability of 0.014 with a corresponding safety index of around 0.59. Because of the epistemic uncertainties underlying the calculated probability of breaching, the distribution (or histogram) of the corresponding annual probability can be similarly obtained. From the histogram of the annual probability of breaching, the corresponding histogram of the safety index can also be generated as shown in Figure 1.8 in which the 90 percent value of the safety index is 1.28.

We might point out that by selecting the 90 percent value of the safety index for the structural design of the levee system, there is reasonably high confidence (so to speak) that the retrofitted 12-ft. levees can withstand the forces of a Category 4 hurricane. Observe that the corresponding median (50 percent) value of the safety index would only be 0.59, which would clearly be too low.

Information and Advice for Decision-Makers

Technical information obtained or generated from a QRA should be presented to the relevant stakeholders or decision makers, in terms of the quantitative risk measures obtained as illustrated above, as well as of the benefit that can accrue from a given investment to reduce each of the respective risks. It is essential that this information be presented to decision-makers who are responsible for allocating resources for minimizing risks. In the case of a natural hazard, the most important risk measures would include the fatality and injury risks, and the risk of economic losses, with the respective uncertainties as represented by the corresponding distributions. From these distributions, the respective risk-averse measures may also be presented to allow the decision-maker the opportunity or option to select appropriate measures depending on his/her personal risk averseness.

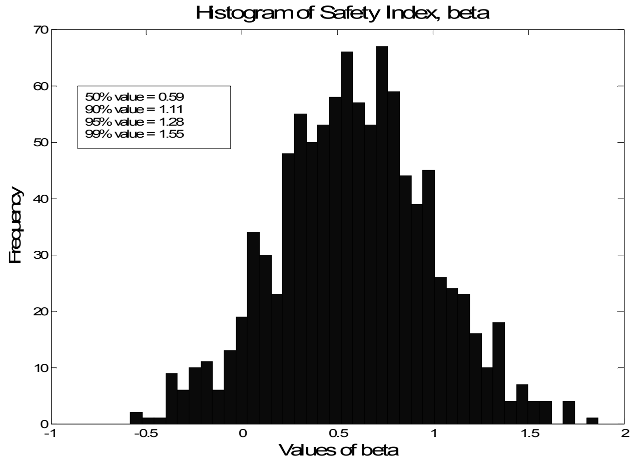

Fig. 1.8. Histogram of safety index, beta

Information and advice presented in quantitative terms, based on the expertise of engineers, should generally be more complete and meaningful to decision-makers. These may be in terms of the best estimate value of the pertinent risk or the complete range (with distribution) of all possible risk measures associated with its epistemic uncertainty. From this distribution risk-averse values may be specified to reduce the effects of the uncertainties underlying the estimated risks. As with other technical information developed for engineering purposes, which are invariably in quantitative terms, risk measures should and can also be developed in the same terms. Society would generally expect such information (that is, supported by quantitative analyses) from the expertise of the engineering community.

Summary and Concluding Remarks

This chapter summarizes the fundamentals for the systematic and quantitative assessment of risk in engineering, with particular emphasis for hazard mitigation. Besides the assessment of the best estimate measure of a pertinent risk, the assessment of the complete range (or distribution) of the possible risk measures is equally important. These are illustrated with a quantitative assessment of the risks (for a 20-year period) associated with the occurrence of a Category 4 hurricane in New Orleans on the assumption that the assessment was performed in 1990 (15 years prior to the occurrence of Katrina in 2005).

The fundamentals of QRA, as summarized and illustrated here, show that QRA is a valuable and practical tool available for engineers to generate quantitative technical information on risk and its associated uncertainty. A conservative (or risk-averse) measure of risk may be specified to reduce the effect of the underlying (epistemic) uncertainty.

QRA can also be used to assess the benefit in risk reduction accruable from an incremental investment and, thus, provide a quantitative basis for risk-benefit study that may be essential and useful for making risk-informed optimal decisions.

QRA is useful and relevant also for developing optimal designs of civil infrastructure systems, including the development of designs based on whole life cost consideration.

Civil engineers, in particular, have the primary responsibility for the design and planning of civil infrastructures, including protective systems to minimize losses of lives and economies during extreme hazard events. In this light, there is every reason that practicing civil engineers should be equipped with the tools of QRA, especially when dealing with problems involving extreme hazards, natural or man-made.

References

A. H-S. Ang and D. De Leon, "Modeling and Analysis of Uncertainties for Risk-Informed Decisions in Infrastructures Engineering," Structure and Infrastructure Engineering, Vol. 1, No. 1, Taylor & Francis, March 2005.

Ang, A. H-S., "Practical Assessments of Risk and Its Uncertainty," IFIP WG 7.3 Working Group Conf. Proc., Taylor & Francis Publishers, Netherlands, 2006a.

Ang, A. H-S., "Optimal Risk-Based Life-Cycle Cost Design of Infrastructures," Proc., LCC5 Workshop, Taylor & Francis Publishers, Netherlands, 2006b.

Ang, A. H-S., and Tang, W.H., *Probability Concepts in Engineering*, 2nd Edition, John Wiley & Sons, Inc, New York, 2007.

Cornell, C.A., "Engineering Seismic Risk Analysis," *Bull. of Seismological Soc. of America,* Vol. 58, 1968.

Der Kiureghian, A., and Ang, A. H-S., "A Fault Rupture Model for Seismic Risk Analysis," *Bull. of Seismological Soc. of America,* Vol. 67, 1977.

Gumbel, E.J., Statistical Theory of Extreme Values and Some Practical Applications," *Applied Mathematics,* Series 33, National Bureau of Standards, Washington, DC, 1954.

Harmsen, S., "PSHA Uncertainty Analysis: Applications to the CEUS and the Pacific NW," *Infrastructure Risk Management Processes,* Ed. C. Taylor and E. VanMarcke, ASCE, 2005, pp.15-63.

Wen, Y.K., and Chu, S.L., "Tornado Risk and Design Wind Speed," *Proc. of ASCE, Jour. of Structural Div.*, Vol. 99, No. ST 12, 1973.

Chapter 2: Quantitative Risk Analysis Applied to Dams

By Erik Vanmarcke, Princeton University

Abstract

The value and use of probabilistic risk assessment are explored, with a focus on an action-oriented approach to decision-making applicable to (systems of) dams, in which the engineer estimates dam failure risks and their consequences and quantifies the effectiveness and economic benefits of alternative strategies aimed at risk reduction.

Risk-Based Decision Analysis

Risk-based decision analysis applied to civil infrastructure systems provides a framework for engineers to identify the kinds and degrees of risk involved in a system or project and the consequences should failure occur. It also and evaluates the effectiveness of alternative actions (for example, in site exploration, design, construction, or monitoring) aimed at controlling or reducing risk. The references cited give examples, involving groups of bridges (Erickson et al. 1989; Cesare et al. 1993, 1994) and dams (Bohnenblust and Vanmarcke 1982 a & b) of the methodology outlined in this chapter. In the case of dams, in particular, the failure event is uncontrolled loss of reservoir contents.

Elements in the Analysis

Relative (or Fractional) Risks

Consider an existing dam whose annual failure risk, p, is expressed as a sum of contributions due to each of the causative hazards (or failure modes), $j = 1, 2, \ldots$

$$p = \sum p_j \tag{2-1}$$

where p_j denotes the annual risk of failure due to hazard j. All possible failure modes must be represented in the summation; this is achievable by lumping all unknown or unidentified causes of failure into a single category labeled "miscellaneous hazards." The summation of probabilities implies that hazards must be defined so as to be mutually exclusive; simultaneously occurring hazards need to be defined as a separate category. (Note: In fault tree theory, Eq. 2-1 can be interpreted in terms of "minimal cut sets.")

Note that the relative (or fractional) risks p_j/p (where $j = 1, 2, \ldots$) sum to one; each value p_j/p is the likelihood that failure, if it occurs, will be caused by hazard j. The basis for estimating these relative risks may be a combination of data on past failures or incidents, professional judgment, and project-specific information (for example, inspection reports).

For instance, in the case of an existing earth dam (Vanmarcke 1974), system failure—sudden release of the contents of the reservoir—may be caused by overtopping, piping (or internal erosion), sliding (not earthquake-related), earthquake-induced sliding, and miscellaneous hazards, for a total of five hazard categories, $j = 1, 2, ..., 5$. The relative risks should be similar for older, non-engineered earthen dams located in a region with moderate earthquake activity.

Reference Alternative, Consequences, and Risk Cost

In analyzing the benefits of actions aimed at risk reduction, it is useful to express both costs and risks in relation to an existing "as is" (*status quo*) condition; this reference "do nothing" alternative involves some (often poorly known) annual occurrence probability, p. Let C_m denote the expected monetary loss if failure occurs; the product $C_m p$ is the annual "risk cost," that is, the expected annual loss due to (possible) failure. It makes sense, in some cases, to assume that C_m is the same regardless of which hazard causes the failure and that protective actions will affect only p, not C_m. For an existing dam, C_m is the estimated economic loss (at the dam site and downstream) in the event of dam failure.

Effectiveness of Mitigating Actions

Engineers have little experience with quantifying the benefits of added protection as these take the form of reduced failure risk and reduced potential losses. Denoting the failure probability (per year) with and without added protection by p^* and p, respectively, we can define the "risk reduction effectiveness" r by means of the relationship

$$p^* = p(1 - r) \tag{2-2}$$

where r is the fraction of the reference-action risk p that is eliminated by the mitigating action. In particular, $r = 0$ means the action is totally ineffective, as it implies $p^* = p$; there is no change in the risk. The value $r = 1$ indicates 100% effectiveness; the risk is eliminated ($p^* = 0$). An action for which $r = 0.9$ reduces the risk by an order of magnitude. A negative value of r implies $p^* > p$; the action increases the level of risk.

Specific mitigating actions often aim at limiting the risk posed by a specific hazard, for instance, raising the crest of a dam reduces the overtopping risk, while adding a protective berm aims at reducing the probability of embankment sliding. The implication is that the effectiveness of mitigating actions is most easily and understandably quantified for specific types of hazards. To capitalize on this, it is useful to express the new risk p^*, like p itself, as a sum of contributions due to all the failure causes $j = 1, 2, \ldots$, as follows:

$$p^* = \sum_j p_j^* = \sum_j p_j (1 - r_j) \tag{2-3}$$

where p_j^* denotes the (estimated) risk due to hazard j if the mitigating action is taken, and r_j is the action's effectiveness in reducing the risk due to causative hazard j. (By definition, $r = r_j = 0$ for the "do nothing" action). The overall effectiveness index r can then be expressed as a weighted combination of the r_j values and the relative risks p_j/p:

$$r = \sum_j (p_j/p)\, r_j. \tag{2-4}$$

To achieve higher overall risk reduction effectiveness r, available funds should be spent on mitigation of hazards for which fractional risks p_j/p are high, and on actions yielding high corresponding effectiveness indices r_j. Estimating those values (for both p_j/p and r_j) will generally require a combination of professional experience and judgment, data from historic failures and near-failures (attributable to the different hazards), and perhaps also support from classical reliability analysis. Specific actions may be highly effective with respect to a target hazard i, (so that r_i may be close to one), but ineffective with respect to all the other hazards ($r_j \approx 0$ for $j \neq i$). The miscellaneous hazards category, for which any action may be regarded as (most likely) ineffective, then produces an upper bound, which can be evaluated by means of Eq. 2-4 on the overall effectiveness r.

The approach is particularly valuable in case negative values of r_j are involved; that is, when a particular action has negative impact on one or more of the contributions to the overall risk. For instance, raising the crest of an existing earth dam, which a hydrologist may recommend, reduces the risk of overtopping but increases the risk of sliding. Whether this action is justifiable, regardless of cost, will depend on the relative risks of overtopping and sliding and the values of the corresponding effectiveness indices (r_j). More specifically, heightening the crest of a dam (without also adding a berm) protects against overtopping ($r_1 > 0$) but worsens the dam's stability ($r_2 < 0$). If the two relative risks are judged to be the same, $p_1/p = p_2/p$, and there happen to be no other significant contributions to the overall risk of failure, then the overall effectiveness r will be negative in case $r_1 < - r_2$. For instance, raising the crest might reduce the hydrologic risk by 90%, but if it doubles the risk of sliding, overall risk reduction effectiveness r will be negative.

The analysis clearly invites interdisciplinary communication between hydrologists and geo-engineers in the case just mentioned in the interest of balanced hazard mitigation. The common way of pursuing safety, based on discipline-specific guidelines, however well intended, may lead to wasteful spending and underachievement in risk reduction.

Expected Benefit

The average annual monetary losses with and without added protection are $C_m p^*$ and $C_m p$, respectively, and their difference is the annual average economic benefit of the risk mitigation strategy.

$$b = C_m p - C_m p^* = C_m pr \qquad (2\text{-}5)$$

In words, b is the product of the *status quo* risk p, the hazard potential C_m, and the strategy's overall effectiveness index r.

Added Cost for Mitigation

The last element in the analysis—the one probably most familiar to decision makers—is the cost of providing added protection. Each action or strategy is characterized by an added-cost-per-year Δc. (Given a discount rate and a time horizon, capital expenditures can also be expressed as an annual disbursement Δc, like a mortgage payment.)

Basic Format of the Analysis

The effectiveness index r and the annualized added cost Δc (or some equivalent cost index) must be evaluated for each action/strategy. A simple (fractional effectiveness) *matrix* whose elements are the measures of fractional or hazard-specific effectiveness r_{jk} of each mitigating action k in reducing the risk due to hazard j can be constructed. The matrix has one column for each hazard ($j = 1, 2, ...$); these are listed on top of each column, along with the corresponding relative risk (p_j/p). These quantities must, of course sum, to 1: $\sum_j (p_j/p) = 1$.

For each (new) mitigating action, one row is added to the matrix. Using Eq. 2-4, the overall effectiveness $r \equiv r_k$ can be obtained for each alternative k. The best action, on an expected cost basis, is that which maximizes the expected net benefit $[b - \Delta c]_k$. Also, any action for which $[b - \Delta c]_k$ is positive, is preferable to the do nothing alternative. It is further useful to plot the quantities b_k, Δc_k, and $[b - \Delta c]_k$ (for each action k) against the action's overall effectiveness r_k and take note of the value of r_k that maximizes $[b - \Delta c]_k$.

The do nothing alternative costs nothing initially ($\Delta c = 0$) but also brings no (annual expected) benefit ($b = 0$, since $r = 0$); it may have high annual future expected cost ($C_m p^* = C_m p$). On the opposite side of the effectiveness scale, achieving a value such as $r = 0.99$ may be prohibitively expensive, or in case there are unknown/miscellaneous cause risks for which $p_j/p > 0.01$, impossible (given the state of knowledge). As mentioned earlier, if an action's overall effectiveness r, evaluated by means of Eq. 2-4, is negative, then that action should not be taken, regardless of cost.

Important Extensions of the Basic Format

"Risk Cost" Format

In general, failure consequences may depend on the (type of) hazard j and may change as a result of mitigating actions taken. Instead of doing the analysis in terms of probabilities p_j and p, it is then more productive to replace the latter by the "risk costs," respectively $q_j \equiv p_j\, C_{m,j}$, the risk cost for hazard j, and q, defined as the sum (over all j) of all these hazard-specific values. The risk-cost ratios, q_j/q, whose sum is 1, now play the same role as the relative risks (and become identical to them if $C_{m,j} = C_m$ for all j). All indices of effectiveness now reflect the impact on risk costs, but the analysis format remains the same: the p's are all replaced by q's in Eq. 2-1 through Eq. 2-4.

Non-Monetary Consequences

The methodology can also be used to quantify benefits of hazard mitigation measures in terms of lives saved (or injuries prevented); the monetary consequences of failure, C_m, are replaced by the life loss potential C_l (expected number of fatalities if failure occurs). A warning system at a dam or levee site, for instance, will be aimed mainly at preventing life loss (by providing timely warning); hence, its effectiveness in reducing life loss may be close to 1, while its effectiveness in reducing property loss is close to 0.

Risk-Based Design Decisions

The methodology, in the format presented, applies to risk-based decision-making not only for existing dams but also for new dams. In a design situation, an appropriate reference alternative may be a "standard design" or a "preliminary" or "trial" design. Next design changes are considered—actions that differ from the reference alternative—and their impact on (initial) cost and on risk and consequences of failure are evaluated.

Optimizing Risk Reduction Programs Involving a System of Existing Dams

The methodology can be used to help make risk-informed decisions about prioritizing inspection (or maintenance or repair) of a group of dams subjected to a multiplicity of hazards. In what follows, we use the subscript i to refer to a specific dam in the group. The total expected annual economic benefits of a dam safety program can be evaluated by summing the (annual expected) benefits associated with each dam. (The probable annual number of lives saved can be evaluated similarly).

In such cases, it may be reasonable to adopt a (default) value for the average annual risk of failure of a dam—any dam in the group. More generally, based on examination of available performance/failure statistics, probability analysis and engineering judgment, you might refine the estimate by allowing it to depend on structural type, age, and design criteria. For each category of structures for which a set of relative risks is developed, you would then attempt to construct a matrix of values the effectiveness index r_{ij} for every alternative inspection/monitoring/repair strategy considered for that structural category. These values, typically between *0* and *1*, indicate the fractional amounts by which the analyst expects risks to be reduced following implementation of the particular inspection scheme. Most r_{ij} values will be close to 0 (implying the procedure has little impact on the risk) or close to 1 (implying a risk reduction by an order of magnitude or higher).

Given a fixed annual budget for a safety program covering many dams of different types and sizes, a reasonable objective in designing the program, that is, in choosing the mix of mitigating actions to be taken, is to maximize total expected monetary benefits. In the case of dams, however, a sensible alternative is to focus on minimizing overall life-loss potential; better yet, you might attempt multi-objective decision analysis, in which both economic and life-loss consequences are given weight, along with environmental factors.

Conclusions

Risk-based decision-making applied to civil infrastructure systems, such as (groups of) existing dams, seeks to put socio-economic and technical issues into proper focus by organizing information about risks, costs, and potential future losses, both monetary and non-monetary. The methodology presented provides a format for summarizing and accounting for (in the case of dams) data about past dam failures, the relative frequency of various causes of failure, the consequences of failure, and the effectiveness of different risk mitigation measures. It facilitates communication about risk and the costs and benefits of reducing risk among stakeholders in decision situations involving mitigation of hazards; most important, it enables quantifying the benefits of actions aimed primarily at risk reduction. In this broad and varied context, the concepts and tools of quantitative risk analysis appear essential to advancing the art and practice of civil engineering.

References

Cesare, M.A., Santamarina, C., Turkstra, C. and Vanmarcke, E., "Risk-Based Bridge Management: Optimization and Inspection Scheduling", *Canadian Journal of Civil Engineering*, Vol. 21, pp. 897-902, 1994.

Cesare, M.A., Santamarina, C., Turkstra, C. and Vanmarcke, E., "Risk-Based Bridge Management", *Journal of Transportation Engineering*, ASCE, Vol. 119, No. 5, pp. 742-750, 1993.

Erickson, H.L., Mulvey, J.M., and Vanmarcke, "Integrating Expert Systems and Mathematical Programming: An Example in Infrastructure Management", *Annals of Operations Research*, Vol. 21, pp. 275-300, 1989.

Vanmarcke, E., Decision Analysis in Dam Safety Monitoring, *Proc. Eng. Found. Conf. on the Safety of Dams*, Henniker, New Hampshire, ASCE, pp. 127-148, 1974.

Vanmarcke, E. and Bohnenblust, H., "Risk-Based Decision Analysis in Dam Safety," M.I.T. Dept. of Civil Engineering Research Report R82-11, 1982.

Bohnenblust, H. and Vanmarcke, E., "Decision Analysis for Prioritizing Dams for Remedial Measures: A Case Study", M.I.T. Dept. of Civil Engineering Research Report R82-12, 1982.

Chapter 3: Risk Assessment for Wind Hazards

By Nasim Uddin, F.ASCE, Professor, University of Alabama at Birmingham, Alabama, USA

Abstract

Current wind-related quantitative risk assessment methodologies are discussed with examples. Recent research developments on modeling wind speed extremes associated with tropical cyclones and tornadoes are also briefly summarized.

Introduction

Wind is defined as the motion of air relative to the earth's surface. The horizontal component of three-dimensional flow and the near-surface wind phenomenon are the most significant aspects of the hazard. Extreme windstorm events are associated with extratropical and tropical cyclones, winter cyclones, and severe thunderstorms and accompanying mesoscale offspring such as tornados and downbursts. Winds vary from zero at ground level to 200 mph 989 m/s) in the upper atmospheric jet stream at 10 to 13 km (6 to 8 mi.) above the earth's surface. The damaging effects of windstorms associated with hurricanes may extend for distances in excess of 160 km (100 mi.) from the center of storm activity. Isolated wind phenomena in the mountainous western regions have more localized effects. It is difficult to separate the various wind components that cause damage during a windstorm. For example, hurricanes have high wind rotating around the eye of the storm, spawn numerous tornados, and generate severe thunderstorm producing strong, localized down drafts (downbursts and microbursts).

Of all the cyclonic storms that rage across the earth's surface, hurricanes are the most damaging because they bring tremendous amounts of rainfall and extremely high winds covering a wide area. Tornadoes, on the other hand, are the most devastating in terms of intensity or extent of destruction of buildings or other man-made structures. Property damage and loss of life from windstorms are increasing due to a variety of factors. Use of manufactured housing is on upward trend, and this type of structure provides less resistance to wind than conventional construction. Because of continued growth of the population in the coastal areas susceptible to high winds from tropical cyclones, the deteriorating condition of older homes, and the increased use of aluminum-clad mobile homes, the impacts of wind hazards will likely continue to increase. The general design and construction of buildings in many high wind zones do not fully consider wind resistance and its importance to survival.

Quantitative Risk Assessment Methodology

Quantitative risk assessment (QRA) will generally consist of three components: (1) hazard analysis, (2) vulnerability analysis, and (3) consequence analysis. The product of the above three components constitutes the estimated risk, R; that is

$$R=H_z \text{ x } V_u \text{ X } C_q \tag{3-1}$$

where H_z = the result of a probabilistic hazard analysis; V_u = the result of a vulnerability analysis; may be in terms of the probability or fraction of damage to a city; C_q= the estimated potential consequence resulting from the occurrence of the hazard. As there are epistemic uncertainties in estimating or calculating each of the components in Eq. 1, the calculated risk will also contain uncertainty leading to a range (or distribution) of the possible risk measures.

Analysis of Wind Hazard

Hazard analysis involves the determination of the probability of occurrence of a given hazard within a given time window. The following provides a brief summary based on the excerpts from Vanmarcke and Chen (2005).

Estimation of Largest Wind Speeds in Non-Hurricane-Prone Regions

Normal wind gives rise to one of the main loading conditions that structural designers need to consider. For most low-rise buildings, load effects due to normal wind are generally small compared to those caused by earthquakes. However, wind effects often dominate for high-rise structures, which possess relatively large fundamental periods of vibration. Normal wind speed is often seen as the sum of two components—the slowly varying mean wind speed and a rapidly fluctuating (turbulent) component. Since in the design of most regular structures the effects of the mean wind load dominate, it is of practical importance to engineers to predict the annual maximum "mean wind speed." The annual exceedance probability p of a given value (of mean wind speed) x_p is p = Prob(X > x_p) = 1 – F(x_p), where $F(x_p)$ denotes the cumulative distribution function (CDF) of annual maximum mean wind speed. The basic design wind speed (x_p) corresponds to a specified value p of annual exceedance probability. Normal wind with mean speed corresponding to an N-year mean recurrence interval is commonly referred to as "the N-year wind" (Simiu and Scanlan 1996). Clearly, the upper tail of the probability distribution of annual maximum wind speeds is critical to the estimation of the basic design wind speed.

Over the years, several types of probability distributions have been proposed to model extreme wind behavior. The three classical extreme distributions are the Type I (Gumbel) distribution, the Type II (Fréchet) distribution, and the inverse (negative) Weibull distribution. The Fréchet distribution was adopted in the design codes of several countries, including the United States in 1972 (see *American National*

Standard ANSI A58.1 1972), because it is regarded as best fitting non-tornado extreme wind speeds blowing in any direction in regions not subjected to mature hurricane winds. Simiu et al. (1978) suggested, however, based on extensive investigation, that the Gumbel distribution may be a more appropriate model.

A fundamental assumption underlying the classical extreme value distributions is that a large number of observed values are (or can be thought of as) realizations of independent and identical distributed random variables with a common but unknown probability distribution (Galambos 1987; Resnick 1987). It is likely, however, that an array of physical phenomena produces varying levels of these observed values of (annual maximum) wind speed. So, all the observations in combination can hardly be expected to fit a single distribution that accurately predicts future extremes. Also, the classical method of statistics of extremes uses only one datum per period, typically the largest value in each data set covering a single year, so that, say, a 30-year record yields only 30 data points (Dougherty et al. 2003). Clearly, such an amount of the data is not sufficient to estimate the distribution's upper tail reliably. An important defect of the classical (extreme value statistics) methodology is the extrapolation to long-term recurrence, say, a 100-year or 500-year return period wind speed estimated based on short-term data, yielding notably unreliable estimates. The degree of conservatism is reduced as the mean recurrence interval grows (Simiu and Heckert 1998). The insufficient amount of data, according to Simiu and Heckert (1996), provides an argument for adopting the reverse Weibull distribution to fit the data on largest daily wind speeds by the peak over threshold method (Dekkers and de Haan 1989). The basic idea behind this method is that values below the threshold likely do not belong to, or originate from, the same distribution as that describing the highest values, so that the inclusion of the lower values distorts the sought-after peak distribution. Only values high enough so they can be assumed to arise from circumstances that generate extreme conditions should be counted.

Estimation of Wind Speeds During Tornadoes

Tornadoes are observed as funnel-shaped clouds consisting of a vortex of air with maximum tangential speeds ranging between 250km/hr. and 800km/hr. Contrasted to the characteristics of hurricanes, those of tornadoes involve small affected regions, high tangential velocities, short lifetimes, straight propagation paths, and much lower frequencies of occurrence at any given location (Ying & Chang 1970; Fujita 1973). Since Fujita developed the F-Scale in 1971 at the University of Chicago, it has become a widely used and practical way of rating the intensity of a tornado based on the observed damage it has caused, ignoring the width and length of the tornado's path (or other physical characteristics). Allen Pearson, director of the National Weather Service's National Severe Storms Forecast Center, added descriptors to the width and length of a tornado path; the resulting scale is known as the Fujita-Pearson Scale.

Let $P(S)$ denote the risk of a tornado striking a particular location in one year; it is proportional to the regional mean frequency of tornadoes and the mean area of a tornado's land-falling path. In certain applications, it is of interest to estimate the annual probability of occurrence of a tornado with maximum wind speed above a given value v_0 at a location, $P(S, v_0) = P(S)\, P(v_0)$, where $P(v_0)$ denotes the probability that the maximum wind speed in a tornado exceeds v_0. Since the F-Scale is also associated with a range of wind speeds, $P(v_0)$ can be used to express relative frequencies of tornadoes with different values on the F-Scale. Weibull distributions have been used to fit sets of data of tornado wind speeds (Rutch et al. 1992). It deserves mention that the F-Scale-based wind speeds cannot be used or interpreted literally. The wind speed numbers in F-Scale are mere guesses and have not been scientifically verified. Engineering assessments of tornado damage by Minor et al. (1977) questioned the accuracy of the F-Scale-based wind speeds. Marshall (1983) utilized load and resistance statistics to demonstrate how uncertainties in assessing building damage can lead to large errors in assigning F-Scale ratings, especially in the upper ranges of the F-Scale. One of the sources of uncertainty discussed by Rutch et al. (1992) is that only a small portion of the damage area will experience F5 wind speeds, while the rest of the tornado-stricken area presumably experiences something less than F5 speed.

In design against tornadic wind, the first thing a design engineer might want to know is the so-called design wind speed. A good probabilistic model should be able to provide this information, and also reflect the following facts: (1) The geographic proneness of tornado strikes, that is, it is more likely to have a tornado in Tornado Alley than elsewhere, (2) the path area and the maximum wind speed vary among tornadoes, thus they have bearing on the chance of a tornado striking a given point and the maximum wind load it induces, and (3) a large tornado (with a large path area) usually brings a higher wind speed or, in probability terminology, these two variables are correlated.

Estimation of Wind Speeds in Hurricane-Prone Regions

Windstorms, hurricanes in particular, constitute one of the costliest natural hazards in the United States, in recent decades far outpacing earthquakes in total damage (Landsea et al. 1999). For the purpose of assessment of damage and losses due to hurricanes, the mathematical simulation of hurricanes is the most widely accepted approach for estimating wind speeds. The Monte Carlo simulation approach, based on the climatological and physical models, was first described by Russell (1968, 1971). Since that pioneering study, many others have expanded and improved the modeling technique. The basic approach in all these studies is similar: Site-specific statistics of key hurricane parameters are obtained, including the central pressure deficit, radius to maximum winds, heading, translation speed, and coast-crossing position or distance of closest approach. Most studies ignore the details of the non-straight path the hurricane actually follows, and the major differences are associated with the specific physical models used, including the filling rate models and wind field models. Other differences include the size of the region over which the hurricane climatology can be considered uniform (that is, the extent of the area surrounding the site of interest for which the statistical distributions are derived or estimated) and the use of a coast segment crossing approach (Russell 1971; Batts et al. 1980), or a circular sub-region approach (Georgiou et al. 1983, 1985; Neumann 1991; and Vickery and Twisdale 1995b). Once the statistical distributions of these key hurricane parameters are known or assumed, a Monte-Carlo approach is used to sample from each distribution, a mathematical representation of a hurricane is passed along the straight-line path in a way that is consistent with the sampled data, and the simulated wind speeds are recorded. Vickery and Twisdale (2000a & b) developed a new method to model the entire track of the hurricane or tropical storm, beginning with its initiation over the ocean and ending with its final dissipation. In this model, the central pressure is modeled as a function of sea-surface temperature, and the storm heading, translation speed, and such are updated at each 6-hr. point in the storm's history. Linear interpolation is used between the 6-hr. points. This approach allows the storms to curve and to change speed and intensity as they move, and it is able to reproduce the continuously varying statistics associated with central pressure, heading, and such along the U.S. coastline.

Vulnerability Analysis

Vulnerability analysis can be defined as the estimation of the extent and severity of damage to man-made and protective systems. The following vulnerability evaluation demonstrates this using a tornado model based on Wen et al (1973).

Suppose the design wind speed for a structure is set at V_o, that is, if this wind speed is exceeded, the structure will suffer some degree of damage, which may range from unserviceability to collapse, depending on the value of V_o. The task, then, is to find the probability or risk level of a tornado striking the point where the structure is located with a maximum wind speed exceeding, V_o, during the entire service life of structure.

Based on the field observations and pioneering works on tornado intensity, Wen et al. derived the following expression for P_n (V_o), which is the probability of tornado striking a given point with a maximum wind speed exceeding V_o during a period of n years.

$$P_n(V_o) = \lambda n R'(V_o) \tag{3-2}$$

The value of λ is the average rate of occurrence of tornadoes and is given in the number of occurrences per square mile-year; λ varies from location to location. Term $R'(V_o)$ is a function determined by the tornado characteristics and their variability; thus $R'(V_o)$ is generally insensitive to change of location. Since $R'(V_o)$ represents the effective area exposed to the wind with a speed higher than V_o during a tornado strike, it is refereed to as tornado speed area function. The curve in Figure 3.1 is fitted by the following equation:

$$R'(V_o) = \frac{1.65}{(1+0.4x10^{-11}V_o^5)^{3/4}} \text{ for } V_o < 290 \text{ mph (467 km/hr.)} \tag{3-3a}$$

$$R'(V_o) = 17.4\exp(-0.014V_o) \text{ for Vo.290 mph} \tag{3-3b}$$

Note also that the first derivative of $R'(V_o)$ is continuous at V_0 = 290 mph. Thus using the above equation, one can obtain a continuous probability density function of V_o.

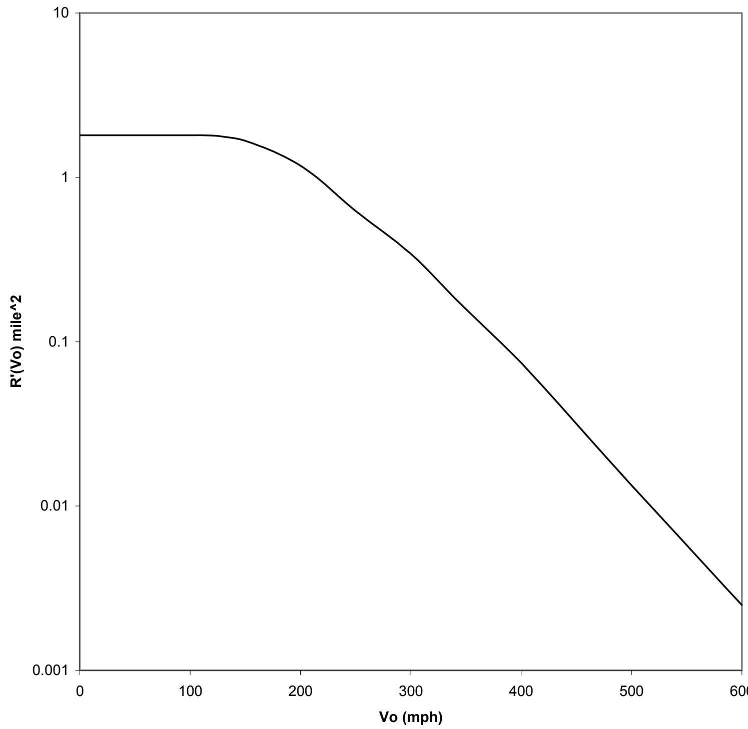

Fig. 3.1. Tornado Speed Area Function, $R(V_o)$

The results derived from the analytical model can be applied to design. Suppose a structure to be built at a certain location Site A. It is desirable to find the design wind speed for a prescribed recurrence interval (or risk level, since probability of a certain wind speed being exceeded in a given year is the reciprocal of recurrence interval) or conversely, the risks of damage to or failure of structure based on a certain design criteria. The procedure can be described by introducing a chart shown in Figure 3.2. The abscissa is annual maximum wind velocity. The vertical scale on the left refers to the probability of such wind speed being exceeded and the scale on the right denotes recurrence interval in years. The dashed straight line is the probability distribution of extreme, nontornadic wind. The analytical expression for this distribution is given by the Frechet distribution

$$F(V_o) = 1 - \exp[-(\tfrac{V}{\beta_2})^{-\gamma}] \tag{3-4}$$

in which γ and β_2 =the scale and shape parameters; γ found to be close to 9.0 for extratropical storms, which are assumed to prevail in Site A. Using γ=9.0, β_2= 50.6 mph (81.5 km/hr.) gives an 85-mph (140 km/hr.) wind corresponding to a 100-year recurrence interval. The dashed curve represents the probability of Site A being struck by tornado in a given year with a maximum wind speed exceeding the abscissa value (including both rotational and translational speed of the tornado). The combined distribution (solid line) is approximately equal to the sum of the two distributions.

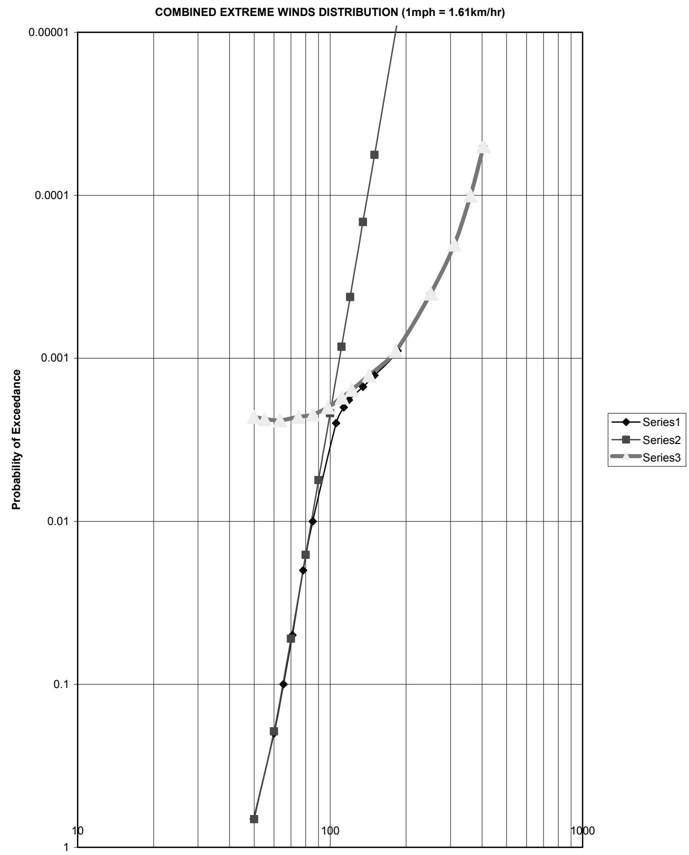

Fig. 3.2. Extreme Wind Distribution (Wen et al. 1973)

(Note that the probability of union of two events, in this case the combined distribution, is approximately equal to the sum of the probability of the individual events, if the probability of their intersection is small).

Suppose the design criterion is that the structure resist a 100-year wind (nontornadic) based on a working stress design. We want to investigate the risk involved in this design and the effects of tornado being taken into consideration. The detailed description of the analyses can be found elsewhere (Gurfinkel and Walser 1972). The maximum net tensile stress caused by a 100-year wind, according to ASCE lateral wind pressure distribution, is found to be the meriodional at El. 120 ft. (37 m) N_φ=35.3 kips/ft. (52,400 kg/m) (due to wind) – 16.3 kips/ft. (24,000 kg/m) (due to self weight) = 19.0 kips/ft. (28,400 kg/m). The meriodional stress due to wind necessary to cause the tower yield is N_φ= 19.0x2.5+16.3=63.8 kips/ft. (94,600 kg/m) in which the factor 2.5 is the ratio of yield stress [60 ksi (42.1 kg/m^2)] to allowable working stress [24 ksi (17 kg/m^2)]. The corresponding wind speed to produce the tensile stress to such a level is 111 mph. Referring to Figure 3.2, the probability of maximum wind speed exceeding 111 mph is 0.002 in a given year (500-year recurrence interval). In other words, risk is that one out of every 500 cooling towers subjected to the identical meteorological conditions will at least yield due to wind load in a given year. Were the possibility of tornado strikes neglected (Fig. 3.2), the probability corresponding to a 111 mph wind being exceeded would be 0.00084 (1,200-year recurrence interval).

The example is based on the design wind approach; stress analysis is that of static and material properties, which and are assumed to be deterministic. A more realistic analysis should examine effects of uncertainties in structural resistance, dynamic response, and the need for a more comprehensive reliability study as shown in the following section.

Consequence Analysis

Consequence analysis is the estimation of the potential consequences caused by the occurrence of the hazard. Near-surface winds and associated pressure effects, positive, negative, and internal, external pressure on structural walls, doors, windows, and roofs, causing the structural components to fail. Positive wind pressure is a direct and frontal assault on a structure, pushing walls, doors, and windows inward. Negative pressure affects the sides and roof where passing currents create lift and suction forces that act to pull building components and surfaces outward. The effects of winds are magnified in the upper level of multi-storied structures. Just as positive and negative forces impact and remove a windward protective building envelop (doors, windows, walls), internal pressures rise and result in roof or leeward building component failures and considerable structural damage or collapse. Debris carried along by extreme winds can directly contribute to loss of life and indirectly to the failure of protective building envelope components. Upon impact, wind-driven debris can rupture a building, allowing more significant positive and internal pressures. Despite its economic prosperity, depth of research enterprise, and breadth of societal infrastructure, windstorm and hurricane-related losses in the United States have escalated to a record $35.8 billion in annual losses during the last five years (NSB 2006). This trend is expected to continue, owing largely to projections of population and housing growth in hurricane-prone regions and recurring above-average seasonal hurricane activity that is expected to occur for the next 10 to 40 years. As an example, from June 1975 to May 1995, 193 federal disaster declarations involved wind-induced natural hazards: 106 for tornados, 40 for hurricanes and tropical storms, 25 for typhoons, and 22 for high winds.

To illustrate consequence analysis a brief, simplified example (e.g., ignoring the time-value of money and assuming hypothetical a New Orleans Category 4 hurricane with a 20 percent probability over a 20-year period), based on Ang (2007), is presented as follows:

Given the occurrence of a particular hazard, there is some chance that structures or infrastructures within the affected zone will be severely damaged or collapsed. This probability, of course, will depend on the distribution of the maximum force from the hazard relative to the capacity of the structures for resisting such forces. As the maximum forces and the structural capacities will both contain variability and uncertainty, each may be represented with a probability model. That is, the maximum forces and structural capacities can be represented with respective random variables and associated probability distributions. For example, we may model the maximum wind speed during a hurricane with a random variable, V, and its probability distribution as a Type I extreme-value distribution shown in Figure 3.3. With the assumption that this is the distribution of the maximum hurricane wind speeds throughout a city or region, the wind resistances of the structures in the city will also vary widely; some can withstand the highest possible speed depicted in Figure 3.3, whereas others could fail under the low end of the speed spectrum of Figure 3.3. We may also postulate that the wind resistances of the structures in the city may be modeled with the lognormal probability distribution of Figure 3.4. On the bases of the probability density functions (PDF's) of Fig. 3.3 and 3.4, we can calculate the probability of failure, pF, of structures (e.g., through Monte Carlo simulation) in the city. The resulting failure probability, pF, may be interpreted as the proportion of structures and infrastructures (buildings, bridges, water tanks, etc) in the city that will suffer serious damage or collapse; in essence, the vulnerability of the city when subjected to a Category i hurricane. An (hypothetical) example is described numerically below to illustrate the conceptual process of QRA as outlined above. In order to clarify the steps in the QRA process, the problem is necessarily idealized, although the assumptions are reasonably realistic. For this purpose, suppose that an analysis of the hurricane risk for New Orleans (for a period of 20 years) was performed 15 years (say in 1990) before the occurrence of Katrina, a Category 4 hurricane, in August 2005. In this illustrative example, the numerical values used are hypothetical and may not be accurate (as they are pre-Katrina). Nevertheless, they serve to illustrate the quantitative process of assessing the underlying risks and associated uncertainties for the purpose of providing the essential quantitative information for making risk-informed decisions for mitigating a future hazard. Assume that upon careful examination of the recorded data on hurricanes in the gulf coast region, the return period of a Category 4 hurricane striking the vicinity of New Orleans is determined to be around 100 years; this means that there is a 1% probability each year, and a 20% probability over a 20-year period, that a Category 4 hurricane can be expected to hit the city of New Orleans and its vicinity. A 20% probability of occurrence over a period of 20 years (which is not particularly long) is a significant probability. A Category 4 hurricane, with a maximum sustained wind speed of 125-145 mph is bound to cause massive damages to ordinary dwellings and severe damages to some of the engineered infrastructures. Except for the engineered infrastructures of reinforced concrete and steel constructions, the ordinary houses would likely be destroyed by sustained wind speeds in excess of 100 mph. Also, as the elevation of the city of New Orleans is 6 to 7 ft. below sea level, the city is protected by the levees and floodwalls that kept the water of the surrounding lakes (such as Pontchartrain) and the Mississippi River from inundating the city. It has been widely reported that the levees were designed and constructed with an average height of around 8 ft for protection against hurricanes of Category 2 or 3. Suppose that the actual levee heights has a symmetric triangular distribution between 7 and 9 ft and that the surges from the lake caused by a Category 4 hurricane can be modeled with a lognormal random variable with an estimated median height of 10 ft and a c.o.v. of

30%. Therefore, under a Category 4 hurricane there is a high probability that the levees will be breached causing massive inundation of the city; with the above assumptions, this probability can be calculated to be as follows: P(levee breached) = 0.78. Furthermore, the vulnerability of much of the houses in New Orleans and vicinity against the hurricane winds would also be very high. Assume that the distribution of sustained wind speed in a Category 4 hurricane is modeled with a Type I extreme-value distribution with a mean speed of 130 mph and a c.o.v. of 40% as portrayed in Figure 3.1, and that the wind speed resistance of houses and other structures is a lognormal random variable with a median of 85 mph and a c.o.v. of 30% as portrayed in Fig. 2. On these bases, the vulnerability of the building stock and other structures in the city to the hurricane winds would be (evaluated through Monte Carlo simulation): Vulnerability of structures = 0.785.

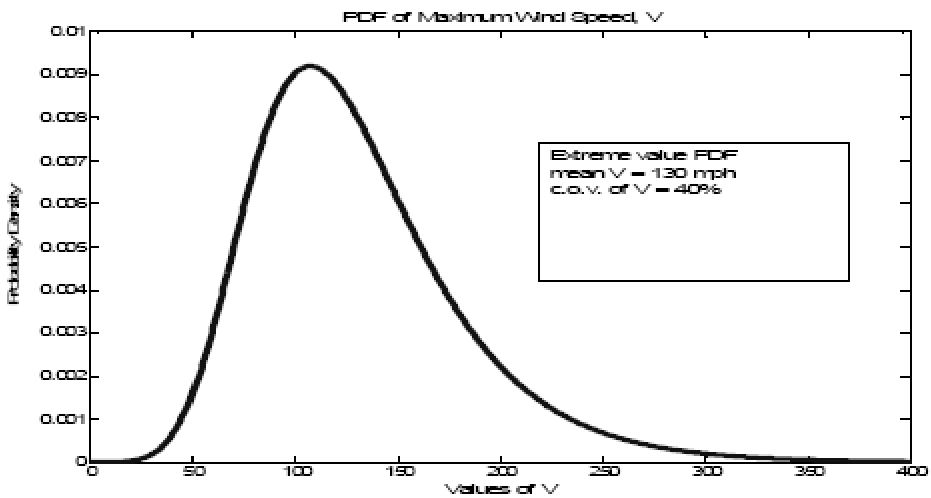

Fig. 3.3. Maximum Hurricane Wind Speed, V

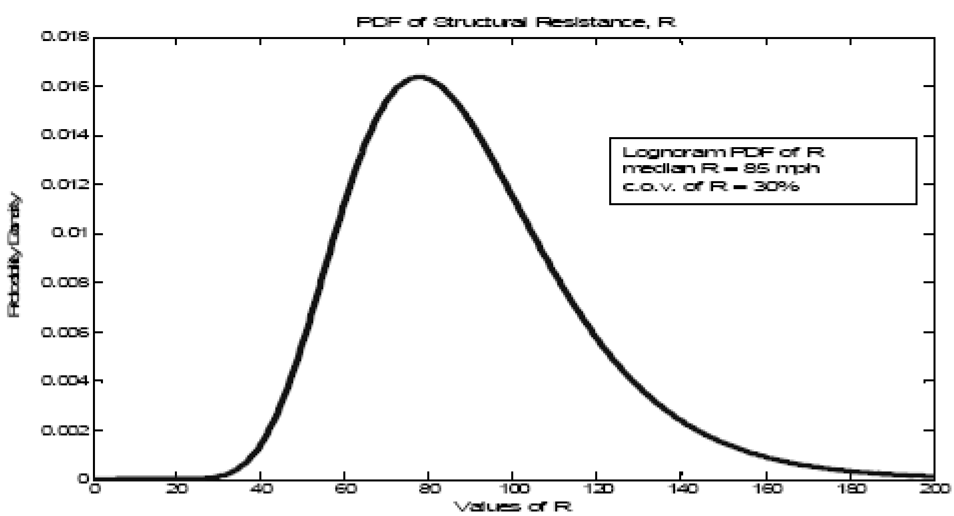

Fig. 3.4. Wind resistance of Buildings, R

The consequences of the destructive effects of a Category 4 hurricane to the city of New Orleans, therefore, must include those caused directly by the high winds as well as by the surges from the lakes. Assuming that up to 90% of the population (approximately 600,000) in New Orleans will be evacuated before the storm, the potential fatalities may be assumed to range from 1,800 to 3,000 (i.e., 3% to 5% of those who did not evacuate) and serious injuries between 5,000 and 10,000, with respective mean values of 2400 fatalities and 7500 injuries; whereas, the economic loss could range between 75 and 150 billion dollars with a mean loss of $112.5 billion. It may be reasonable to assume (prior to the occurrence of Katrina) that the fatalities and injuries will be caused equally by the extreme wind and by the inundation of the city; whereas the economic loss will largely be caused by the failure of the levee system and subsequent inundation of the city. On the basis of the above postulated information, the "best estimate" of the risks to the city of New Orleans can be summarized as follows (based on respective mean values): Fatality risk = 0.5[0.20(0.785)(2400)] + 0.5[0.20(0.78)(2400)] = 376; Risk of serious injuries = 0.5[0.20(0.785)(7500)] + 0.5[0.20(0.78)(7500)] = 1,174; Risk of economic loss (in dollar) = 0.20(0.78)(112.5) = $17.55 billion.

The results of a quantitative risk assessment will permit also a quantitative analysis of the reductions in the respective risks that can accrue from an investment in strategies to mitigate the effects of a future natural hazard. A clear example is the risk reductions accruing from strengthening and raising the height of the levees around New Orleans for protection against a Category 4 hurricane. Suppose that the cost to improve the levee system will be $1.00 billion to insure against or mitigate any inundation of the city. This may require raising the height from the existing average height of 8 ft to a uniform height of 12 ft plus any needed strengthening of the levees and floodwalls. With 12-foot levees, the probability of breaching from a Category 4 hurricane will be reduced to the following: P(levee breached) = 0.27 and the "best estimate" reduced economic risk from inundation would be Reduced economic risk = 0.20(0.27)(112.5) = 6.08 billion dollars The reduced fatality risk would become Reduced fatality risk = 0.5[0.20(0.27)(2400)] + 0.5[0.20(0.785)(2400)] = 253 and the corresponding reduced risk to injuries would be Reduced injury risk = 0.5[0.20(0.27)(7500)] + 0.5[0.20(0.785)(7500)] = 791. Therefore, with the investment of $1.0 billion to improve the levee system, the "best estimate" net reductions in the respective risks would be as follows: reduction in economic risk = (17.55 – 6.08-1.00) = $10.47 billion; reduction in fatality risk = (376 – 253) = 123; and reduction in injury risk = (1174 – 791) = 383, which are significant reductions in the respective risks accruable from the $1.0 billion investment for improving the levee system.

Summary and Conclusions

The insurance industry spent nearly $23 billion on wind-related catastrophic events from 1981 to 1990 (NRC, 1993). Of the three primary sources, hurricanes and tropical storms, severe thunderstorms, and winter storms, severe local windstorms accounted for 51.3 percent of expenditures. Although a number of property loss projection models have been developed, most of them use post-disaster investigations

(FEMA, 1993) or available claim data to fit damage versus peak wind speed 'vulnerability curves'. As pointed out by Pinelli, Simiu, et al. (2004), the most reasonable approach may be to combine the (relatively recent) probabilistic approach to structural damage estimation and the wind field model. Examination of insurance claim files from hurricane Hugo and Andrew revealed that most wind damage to houses is restricted to the envelope of the building. The risk of death and injury from hurricanes is very low, so the main criteria for minimizing insurance company and homeowner losses are economic, i.e., reducing damage to buildings and their contents, instead of related to life-safety. These investigations seek to define damage modes for different types of construction and building materials. Indeed, there are better prospects for sorting damage modes of structures during hurricanes, considering the envelope character of the damage, compared to the more complex patterns of damage and failure of structures during severe earthquakes. Of course, the combined effects of wind and earthquakes are also of great interest to engineers.

References

American National Standard A58.1-1972 (1972), Am. Nat. Standards Inst., New York.

Ang, H-S, "Fundamentals of Quantitative Risk Assessment for Natural Hazard Mitigation," *Disaster Risk Assessment and Mitigation,* Reston, VA: American Society of Civil Engineers, Council on Disaster Risk Management, Monograph No. 2, May 2007.

Batts, M.E.; Cordes, M.R.; Russell, L.R.; Shver, J.R.; and Simiu, E. (1980), Hurricane wind speeds in the United States, Rep. No. Bss124, Nat. Bureau of Standards, U.S., Department of Commerce, Washington, DC.

Dekkers, A.L.M., and de Haan, L. (1989), On the estimation of the extreme-value index and large quantile estimation," Ann. Stat., 17:1795-1932.

Dougherty, A. M.; Corotis, R.B.; and Segurson, A. (2003), Design wind speed prediction, J. Struct. Engrg., 129(9):1268-1274.

Federal Emergency Management Agency (FEMA 1993), "FEMA Disaster Costs."

Fujita, T.T. (1973), Tornadoes around the world, Weatherwise 27:56-62.

Galambos, J. (1987), "The asymptotic theory of extreme order statistics," Kridger, Malabar, FL.

Georgious, P.N., (1985) "Design wind speeds in tropical cyclone-prone regions," Ph.D. thesis, Fac. of Engrg. Sci., University of Western Ontario, London, Ont., Canada.

Georgious, P.N., Davenport, A.G., and Vickery, B.J. (1983), Design wind speeds in regions dominated by tropical cyclones, J.Wind Engrg. and Industrial Aerodynamics, 13(1), 139-152.

Gurfinkel, G., and Walser, A., “Analysis and Design of Hyperbolic Cooling Towers,” Journal of the Power Division, Vol. 98, No. 7, Proc. Paper 8997, ASCE, June 1972, pp. 133-152.

Landsea,C.W.; Pielke, Jr.R.A.; Mestas-Nunez, A.M.; and Knaff, J.A. (1999), “Atlantic Basin Hurricanes: Indices of climatic changes,” Climatic Change, 42,89-129.

Marshall,T.P. (1983), “Utilization of load and resistance statistics in a wind speed assessment,” M.S.thesis, Dept. of Civil Engineering, Texas Tech. University, 91pp.

Minor,J.E. (1977), “Engineered-oriented examinations of the tornado phenomenon.” Preprints, 10th Conf. on Severe Local Storms, Omaha, NE, Amer.Meteor, Soc., 438-445.

National Research Council (NRC 1993), Committee on Assessing the Costs of Natural Disasters, Board on Natural Disasters, and the Commission on Geosciences, Environment, 64 Assessing Federal Research and Development for Hazard Loss Reduction and Resources, The Impacts of Natural Disasters: A Framework for Loss Estimation, Washington, DC: National Academy Press, 1993.

National Science Board (NSB 2006), Science and Engineering Indicators 2006, Arlington, VA: National Science Foundation, 2006.

Neumann, C.J., and McAdie, C.J. (1991), A revised national hurricane center NHC83 model (NHC90), NOAA Tech. Memo, NWS NHC-44,35pp.

Pinelli, J.P.; Simiu, E., et al. (2004), Hurricane damage prediction model for residential structures, J.Struct.Engrg.,130(11):1685-1691.

Resnick, S.I. (1987), Extreme values, regular variation and point processes, Springer, NY.

Russell, L.R. (1971), Probability distribution for hurricane effects, J.Wtrwy., Harb. and Coast. Engrg. Div., ASCE, 97(1):139-154.

Rutch, C.; Anselmo,K.J.; and Linney,R.E., et al. (1992), Tornado risk analysis, Plant/Operations Progress, 11(3):134-139.

Simiu, E. and Heckert, N.A. (1998), Ultimate wind loads and direction effects in non-hurricane and hurricane-prone regions, Environmetrics, 9:433-444.

Simiu, E., and Heckert, N.A. (1996), Extreme wind distribution tails: A peak over threshold approach, J. Struct. Engrg., 122(5):539-547.

Simiu, E. and Scanlan, R.H. (1996), Wind effects on structures: fundamentals and applications to design (3rd edition), New York : John Wiley.

Simiu, E.; Filliben, J.J.; and Biétry, J. (1978), Sampling errors in the estimation of extreme wind speeds, J. Struct. Div., ASCE, 104(3):491-501.

Simiu, E.; Heckert, N.A.; and Whale, M. (1996), Estimation of hurricane wind speeds by the peaks over threshold approach, NIST technical Note No.1416, NIST, Gaithersburg, MD.

Vanmarcke, E. and Chen, Z. "Wind Field Statistics: Literature Review and Research Needs", Proc. of National Science Foundation US-Bangldesh Workshop on Inkovation in wind Strom and Strom Surge Mitigation Construction, December 2005.

Vickery, P.J. and Twisdale L.A. (1995a), Wind-field and filling models for hurricane wind-speed predictions, J. Sturct. Engrg., ASCE, 121(11):1700-1709.

Vickery, P.J. and Twisdale L.A. (1995b), Prediction of hurricane wind speeds in the United States, J. Sturct. Engrg., ASCE, 121(11):1691-1699.

Vickery, P.J.; Skerlj, P.F.; and Twisdale, L.A. (2000b), Hurricane wind field model for use in hurricane simulations, J. Struct. Engrg., 126(10): 1203-1221.

Vickery, P.J.; Skerlj, P.F.; and L.A.Twisdale, (2000a), Simulation of hurricane risk in the U.S. using empirical track model, J. Struct. Engrg., 126(10):1222-1237.

Wen, Y.K. and Chu, S.L., "Tornado Risk and Design Wind Speed," Proc. of ASCE, Jour. of Structural Div., Vol. 99, No. ST 12, December 1973.

Ying, S.J. and Chang, C.C. (1970), *Exploratory Model Study of Tornado-Like Vortex Dynamics*, J. Atmos. Sci., 27:3-14.

Chapter 4: Quantitative Earthquake Risk Assessment

By Anne Kiremidjian[1], Stanford University, Stanford, CA; Evangelos Stergio, Guy Carpenter Inc., New York, NY; and Renee Lee, Arup, San Francisco, CA

Abstract

A brief summary of earthquake risk assessment methods is presented. The method is general and can be applied either to a single structure or to a group of structures that are spatially distributed in a region exposed to earthquakes. Furthermore, lifeline systems, such as water, power, communications, and transportation system, can be analyzed with the method presented here but with consideration of the network flow through the system. For either a single structure or a distributed system, the risk can be due to direct damage or to loss of functionality. The application of this method to a transportation network system within the San Francisco Bay Region is demonstrated by an example.

Introduction

Recent earthquakes, such as the 1994 Northridge, California, and the 1995 Kobe, Japan events, showed that damage to structures can result in large losses to individual owners and to a community. The significance of functionality losses, resulting from the closure of building, facilities, or lifeline systems, was also amply demonstrated. Both of these types of losses point to the need for a detailed and systematic risk assessment approach. In this paper, a general framework for earthquake risk analysis of individual structures or lifeline systems is presented with specific consideration of direct damage and down time. Results from a recent project supported by the Pacific Earthquake Engineering Research Center (PEER) on transpiration systems are presented to illustrate the method.

Earthquake Risk Assessment Overview

Structure Risk Assessment

Seismic risk assessment methods have been developed over the past 30 years and are now reaching a level of acceptance by the general engineering community as viable method for design and decision-making. In this paper we follow the formulation proposed by PEER. For individual structures (and these can be components of a lifeline system) the risk is measured in terms of a decision variable, DV. The risk to a structure is given by

$$P[DV > dv] = \iiiint dF_{DV|DM} \, dF_{DM|EDP} \, dF_{EDP|IM} \, dF_{IM} \qquad (4\text{-}1)$$

where

DV = the decision variable

DM = the damage measure

EDP = the engineering demand parameter

IM = the intensity measure

F = the cumulative distribution of the random variable.

IM in Eq. 4-1 can be either a single variable or a vector of variables. It can represent ground motion at the site of a network component or a ground deformation measure. The most commonly used ground motion *IM*s are peak ground acceleration and spectral acceleration. Ground deformation *IM*s represent the amount of lateral spreading and/or settlement at a site. *IM*s are obtained through conventional probabilistic seismic hazard analysis expressed as the annual probability of exceedence of the *IM* at a location. To account for ground motion and ground deformation, the following formulation is developed (Kiremidjian et al. 2006):

$$\begin{aligned} P[DV \geq dv] &= I_A \iiiint dF_{DV|DM} \, dF_{DM|EDP} \, dF_{EDP|IM} \, dF_{IM} \\ &+ I_L \iiiint dF_{DV|DM} \, dF_{DM|EDP} \, dF_{EDP|IM=S_H} \, dF_{IM=S_H} \\ &+ I_L \iiiint dF_{DV|DM} \, dF_{DM|EDP} \, dF_{EDP|IM=S_V} \, dF_{IM=S_V} \end{aligned} \qquad (4\text{-}2)$$

where,

$$I_A = \begin{cases} 1 \quad \textit{if there is no liquefaction, or landslide,} \\ \textit{or fault rupture at a site} \\ \\ 0 \quad \textit{if there is liquefaction or} \\ \textit{landslide or fault rupture at a site} \end{cases} \qquad (4\text{-}3)$$

$$I_L = \begin{cases} 1 \quad \text{if there is liquefaction or landslides} \\ \text{or fault rupture at a site} \\ \\ 0 \quad \text{if there is no liquefaction or landslide} \\ \text{or fault rupture at a site} \end{cases} \tag{4-4}$$

A = ground motion severity

S_H = horizontal ground displacement due to either liquefaction or landslides or to differential fault displacement

S_V = vertical ground displacement due to either liquefaction or landslides or differential fault displacement.

It is assumed in this formulation that either liquefaction, landslides, or differential fault displacement from fault rupture occur at a site but none simultaneously. Similarly, if there is either liquefaction or landslide or fault displacement, they govern the damage and any damage due to ground shaking alone is considered to be already included in the ground deformation analysis.

Given the *IM,* the engineering demand parameter (*EDP*) is evaluated in terms of structural response measures such as deformations, accelerations, induced forces, or other appropriate quantities. Relationships between *EDP* and *IM* are obtained through inelastic simulations, implementing structural, geotechnical, and nonstructural damage models. The *EDPs* are then related to damage measures (*DM*), which describe the physical damage. The *DMs* include descriptions of damage to structural elements, non-structural elements, and contents, in order to quantify the necessary repairs along with functional or life safety implications of the damage. Specifically for building or bridges, *DM* describes the damage to their structural elements or the structural system. The final step in the assessment is to calculate the decision variables, *DV*, in terms of mean annual probabilities of exceedance, $v(DV)$. In general, the *DVs* relate to one of the three decision metrics that include direct dollar losses, downtime (or restoration time), and casualties. The *DVs* are determined by integrating the conditional probabilities of *DV* given *DM,* $p[DV{=}dv|DM]$, with the mean annual *DM* probability of exceedance, $v[DM]$.

Lifeline Network Risk Assessment

The PEER methodology is limited to estimating the risk to components of a lifeline system. In this section we present the network risk estimation method as it pertains to transportation systems. Damage to the components of the network often results in the closure of specific links until these components are repaired. This action increases the level of traffic congestion and travel time or reduces the number of trips taken. For other networks, such as water systems, closure of a component will result in reduced flow to a terminal point. Trip or flow reduction is very difficult to predict; however, logical estimates can be made given the socio-economic profile of the area of study.

The increase in travel time can be found with respect to a baseline scenario. Travel time delay, however, is highly correlated to the number of trips that are lost. The problem of the risk assessment of a transportation network becomes more complex under this approach because the indirect loss has two components, the cost of the delays and the cost of the lost trips.

To develop a network risk assessment model, it is necessary first to formulate a network flow model. For transportation networks, a traffic assignment model allocates the traffic within the network components based on the supply and the demand for trips. For other flow networks, the volume and pressure of the flow needs to be specified for each link. The results of such an analysis are the flow (for example, number of cars or flow volume and pressure) and the time needed to travel through each component. Traffic flow models were utilized by Cho, Fan, and Moore (2003) and are summarized in the highway demonstration project (Kiremidjian et al. 2006) and will be used in the illustration that follows in this paper.

Estimation of Total Risk

The risk can be expressed as the expected loss or the probability of exceeding a loss level. For spatially distributed systems, estimation of the probability of exceeding loss level can be particularly challenging because components of the system are subjected to different ground motions with each earthquake event. Most frequently, a simulation approach is used to estimate the loss to a system where component and functionality loss is evaluated for each event and then the contribution of loss from all events is combined for a total risk formulation. In the following subsections, we first address the estimation of expected loss and the uncertainty of that loss, referred to as point estimates of loss and then discuss the total risk curve analysis.

1.1 General formulation of point estimates of loss

The total expected loss for a given event is given by the following equation:

$$E(L \mid Q) = \int l_s f_{L_s|Q}(l_s|Q)dl_s + \int l_n f_{L_n|Q}(l_n|Q)dl_n \qquad (4\text{-}5)$$

where

L_s = the structural loss of the components

Q = the scenario event

L_n = the loss due to network disruption

F = the probability density function of the random variable

E(L|Q = the expected value of loss L given the event Q

In Eq. 4-5 the decision variable *DV* has been expressed in terms of monetary loss *L*. The event *Q* is defined by its magnitude, rupture length and location, rupture depth, and dip angle of fault. With these specifications, the *IM* is estimated for events with rate ν_i at all bridge sites. The structural loss is evaluated based on the PEER methodology discussed in the previous section. The operational loss in the same equation requires a network analysis model with traffic assignments for the region presented in the preceding section. It implies that traffic delays *D* on various links of the system are first computed and then the losses L_n are estimated as function of the operational losses due to that time delay *D*.

The annualized risk for the system from all possible events that occur with rate ν_i is expressed in the following equation:

$$\nu(L) = \sum_{\text{all events}} \nu_i * \left\{ \begin{array}{l} \displaystyle\sum_{\substack{\text{all network}\\ \text{components}}} \int l_s f_{L_s|Q}(l_s \mid Q) dl_s + \\ \displaystyle\int l_n f_{L_n|Q}(l_n \mid Q) dl_n \end{array} \right\} \tag{4-6}$$

where

L_s = the structural loss of the components

Q = the scenario event

L_n = the loss due to network disruption

$f_X(x)$ = the probability density function of the random variable

ν = the annual rate of occurrence of an event or the rate of *DV* = total loss *L*

Eq. 4-6 cannot be expressed in closed form and is evaluated numerically or through simulation. For large networks, the analytical complexity can be challenging and computational run-times can be excessive. Several methods have been proposed for efficient computation of the multiple integrals of Eq. 4-1 and 4-2, which are implicitly contained in Eq. 4-6. Also implicit in this equation is the aggregation of loss from all network components. This aggregation is further discussed in the next section.

Point Estimates of the Structural Loss for Multiple Sites and Single Event

For network systems the risk estimates are applicable to multiple components to make decisions for retrofitting strategies or planning new links. In this section, we will generalize the two methods to estimate the loss at a single site and apply them to a set of components. In the development that follows, the dependence on the event Q is dropped to simplify the notation.

The loss from n components in a network is the sum of n random variables. According to probability theory, the sum of the expected values of the loss of all the components will be equal to the expected value of the total loss. The variance of the total loss is equal to the sum of the variances, under the assumption that the damage of the components is uncorrelated. The equations follow:

$$E(Total\ Loss) = \sum_{all\ components} \{E(l_i)\}$$
$$\sigma^2 = \sum_{all\ components} \sigma_i^2 \tag{4-7}$$

where

$E(l_i)$ = the expected value of the loss at a single site

σ_i = the variance of the loss at a single site

If the losses, however, are correlated, the variance is given by

$$E[L_{total}] = \sum_{i=1}^{n} E[L_i] \tag{4-8a}$$

$$\sigma_{L_{total}}^2 = \left[\sum_{i=1}^{n} \sigma_{L_i}^2 + \sum_{i=1}^{n} \sum_{\substack{j=1 \\ j \neq i}}^{n} \rho_{L_i L_j} \sigma_{L_i} \sigma_{L_j} \right] \tag{4-8b}$$

where ρ_{ij} is the correlation between loss L_i at site i and loss L_j at site j within the system.

The challenge in evaluating Eq. 4-8b is in estimating the correlations ρ_{ij}. Recent research by Lee and Kiremidjian (2006) has demonstrated that the losses at pairs of bridge sites are correlated through ground motion and bridge damage.

Probability Distributions of the Structural Loss for Multiple Sites and Single Event

In general, the first terms in Eq. 4-5 and 4-6 can be expanded to explicitly show the damage measure *DM*, engineering demand parameter *EDP* and intensity measure *IM* conditional probability density functions. The challenge is in evaluating the probability density function (PDF) of loss for all bridges in the network system for a given event. The challenge is further increased when all possible events are considered. In this section we develop the aggregated loss from structural damage for a single event.

For a given event Q_j, j =1,2,…N, the total loss resulting from damage to components (bridges) of the network is the sum of all the losses. Since the loss of each component is a random variable with its own distribution, the sum of the losses is a convolution of the individual probability density functions. That is,

$$L_{total} = L_1 + L_2 + L_3 + \ldots + L_n \tag{4-9}$$

$$f_{L_{total}} = f_{L_1} \otimes f_{L_2} \otimes f_{L_3} \otimes \ldots \otimes f_{L_n} \tag{4-10}$$

where

L_{total} = the total loss for a set of n bridges

L_i = the loss for bridge i, $i=1,2,\ldots n$ for a given event Q_j

$f_X(x)$ = the PDF of a random variable X

$\otimes$ = the symbol for convolution

In the preceding equations, the subscript referring to the event j is dropped for simplicity of notation. Using the well known property that the convolution in the time domain becomes multiplication in the frequency domain, we can compute the probability density of L_{total} by transforming the network component PDFs of loss, $f_L(l)$, into the frequency domain, multiplying them in the same domain, and then apply the inverse transformations to obtain the probability density in the time domain. To reduce the error in transformation, two PDFs are transformed successively until the variables are exhausted and the total loss PDF is estimated. It is recalled that Eq. 4-9 and 10 are for a given event and the distributions are conditional on that event.

Evaluation of the Network Functionality Loss

Undoubtedly, the network performance drops after an earthquake event because of its decrease in capacity or component closures. To quantify this reduction in functionality we first estimate the expected value of the operational loss of the network relative to a baseline performance, which is the performance prior to the earthquake. Then the uncertainty on that loss can be computed considering various sources of variability in the system.

Expected Value of Network Functionality Loss

Damage to network components defines the reduction in flow capacity. For example, a bridge with 20% damage will have to reduce its traffic by the same percentage to meet its demand. When the damage exceeds 40%, we assume that the bridge is closed and passengers have to make a detour.

Travel time delays are estimated by subtracting baseline travel times from the travel times in the network with reduced capacity. It is possible to convert this delay to monetary units, if we know the value of time and the number of passengers.

Component repair duration will depend on the damage level of the bridge and will vary for each bridge type. In order to have a realistic assessment of the total operational loss, estimates for restoration times are obtained for the different damage states. Network performance analyses are conducted immediately after the event and again after 1, 3, 7, 14, 30, 180 and 365 days. The total indirect loss is then the integral of this curve and must be added to the structural loss in order to estimate the total loss of the scenario. This operation represents the expected value of functionality loss for the lifeline network.

Transportation Network Risk Curve from Monte Carlo Simulation with Importance Sampling

Evaluation of Eq. 4-6, which leads to the total risk curve, is computationally very expensive. In general, there are three methods to compute Eq. 4-6: (1) numerical integration, (2) conventional Monte Carlo simulations, and (3) Monte Carlo simulation with importance sampling. Numerical integration considers the full assessment of the equations describing the risk model. Monte Carlo simulation is an approximate method that randomly selects scenarios over time and evaluates the loss rate curve. It must be repeated many times to obtain stable results or it needs to be run over long forecast periods to capture all possible events. Importance sampling is again a simulation-based approach that selects a combination of scenario events in the region in such a way that the mean and higher order moments of the risk rate curve are preserved with the minimum number of scenarios.

Considering the nature of the transportation network problem, analytical methods cannot be used for risk assessment. Thus, we choose the importance sampling method because it minimizes the analyses while preserving important components of the risk curve such as the mean and at least the second order moment (variance) of the loss rate. Then the losses from each scenario are combined as follows.

Earthquake events are assumed independent and follow a Poisson process. It is recalled that an event is defined by its magnitude, rupture length, rupture location, rupture depth, dip angle, and annual rate of occurrence. We denote the probability of a scenario event to be $P[Q_j]$, j = 1,2, …N, where Q_j is the j^{th} event that is identified as being important for the risk curve computation and N is the total number of events. If the loss for each scenario Q_j is L_j, j = 1,2,3…N, we order the losses in decreasing order.

$$L_n > L_{n-1} > ... > L_k > ... > L_1 \tag{4-11}$$

Then the probability of exceeding the loss rate in a year is obtained by

$$\mathrm{P}[\mathrm{L}_{\mathrm{k}} \geq l] = 1 - \prod_{j=k}^{n}\left(1 - P[Q_j]\right) \tag{4-12}$$

In Eq. 4-12, the assumptions are made that (1) individual losses are independent, (2) the system is fully restored after each event, and (3) only one event occurs at a time. While this equation is a simplification, it is computationally tractable and provides additional information over expected value loss estimates as will be demonstrated in the application section of this paper.

Application to the San Francisco Bay Bridge Loss Estimation

This paper presents a brief example of computation of losses to a set of bridge in the San Francisco Bay Area. More detailed discussion of network loss analysis and assessment are provided in Stergiou (2006). Damage and loss estimates were obtained for 1,125 bridges that are part of the transportation network system in the region. The bridges were classified in generic structural classes according to the definitions in HAZUS (1999) and fragility functions from the same document were used for estimating the damage to several scenario earthquakes.

The seismicity in the San Francisco Bay Area is dominated by the San Andreas and Hayward faults. Magnitudes, their frequency of occurrence and rupture locations are well documented in a recent report by USGS (2003). For the purposes of our application, earthquakes of moment magnitude, $M_w = 6.75$ are considered to be appropriate lower threshold. The upper threshold values are *8.0* and *7.5* for the San Andreas and Hayward faults, respectively (USGS 2003). Considering various rupture locations along each fault, a total of 56 scenario events are identified and used in the risk assessment. The reader is referred to Stergiou and Kiremidjian (2006) for further detail.

Boore, Joyner, and Fumal's (1997) ground motion attenuation model is used to predict site ground motions. For that purpose the local soil conditions are assessed according to the California Geological Survey (CGS). Ground motions are estimated at each bridge site in the network system with corresponding annual rate of occurrence (that is, an *IM* value with a rate ν_{IM}).

Information on liquefaction susceptibility is obtained from the U.S. Geological Survey Open File Report 00-444 (USGS 2000) and the methodology for liquefaction and landslide analysis provided in HAZUS (1999) is used to estimate liquefaction and landslide ground deformations at bridge locations.

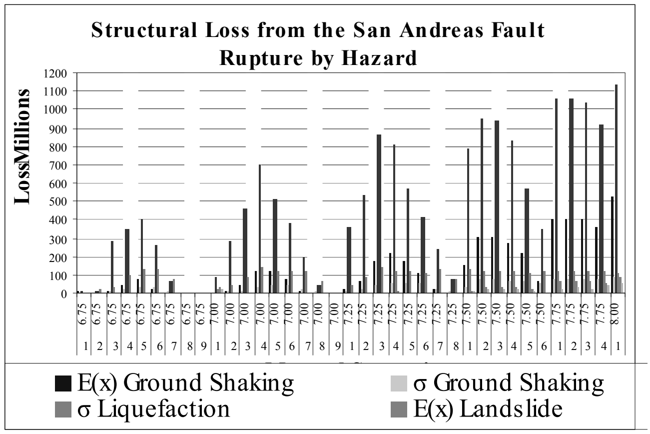

Fig. 4.1. Loss from structural damage to pre-retrofitted bridges

The loss from damage to bridges from each scenario event is estimated by multiplying the expected damage state of a bridge by its replacement value. Figure 4.1 shows the loss from damage to bridges due to ground shaking, liquefaction, and landslides resulting from the potential occurrence of events on the San Andreas Fault. From that figure, the highest losses are from the magnitude 8.0 event on the San Andreas Fault, as expected. The contribution of losses due to liquefaction appears to be twice as large as those due to direct ground shaking. The loss from landslides is small in comparison to ground shaking and liquefaction.

The total replacement cost for the 1,125 bridges considered in this study is estimated to $2,891 million. The total expected value of structural loss reaches a maximum of $1.18 billion for the San Andreas Fault scenarios.

Conclusion

A general formulation for earthquake risk assessment is presented that considers ground motion, liquefaction, and landslide hazards as well as the contribution of direct physical loss and functional loss. Application of the methodology to the San Francisco Bay Area shows that the direct physical loss can be significant. Findings show that liquefaction has the highest influence of all the hazards, but additional research to develop more robust methods of analysis is recommended.

Acknowledgment

The partial support from the Earthquake Engineering Research Centers Program of the National Science Foundation, Award No. EEC-9701568 and from the UPS Foundation Endowment are gratefully acknowledged.

References

Boore D, Joyner W, Fumal T, (1997), Equations for Estimating Horizontal Response Spectra and Peak Acceleration from North American Earthquakes: A Summary of Recent Work, *Seism. Res. Lett*., 687(1), 128-154.

Cho, S. Fan, Y.Y., and Moore, J., (2003). Modelling Transportation Network Flows as a Simultaneous Function of Travel Demand, Network Damage and Network Level Service, *Proceedings of the Sixth Us Conference and Workshop on Lifeline Earthquake Engineering,* ASCE, August 10-13, 2003, Long Beach, CA, pp. 868-877.

HAZUS, (1999). *Earthquake Loss Estimation Technical Manual,* National Institute of Building Sciences, Washington D.C.

Kiremidjian AS, Moore J, Fan YY, Basoz, N., Yazali, O, Williams M, (2006). PEER Center Highway Demonstration Project. PEER 2006/04.

Lee R., Kiremidjian AS, (2006). Uncertainty and Correlation for Loss Assessment of Spatially Distributed Systems, *Earthquake Spectra*, Vol. 23, No. 4, pp. 753-770.

Stergiou E and Kiremidjian AS, (2006). Treatment of uncertainties in seismic risk analysis of transportation systems, *The John A. Blume Earthquake Engineering Center, Report No. 156*, Stanford University,

USGS, (2000). Preliminary maps of quaternary deposits and liquefaction susceptibility, nine-county San Francisco Bay Region, California: a digital database – Open File Report 00-444, [http://geopubs.wr.usgs.gov/open-file/of00-444/].

USGS, (2003). Earthquake Probabilities in the San Francisco Bay Region: 2002–2031, Open-File Report 03-214, [http://pubs.usgs.gov/of/2003/of03-214/]

Chapter 5: Risk Assessment for Bridge Decision-Making

By Dan M. Frangopol, Lehigh University, Bethlehem, PA, and Thomas B. Messervey, United States Military Academy at West Point, NY

Abstract

This paper investigates how the inclusion of risk can enhance the design, assessment, and management of bridge structures. Similarities are investigated between the risk-based decision-making process and reliability-based life-cycle management (LCM) methods with the intent of combining synergistic benefits from each approach. A pre-posterior analysis in a Bayesian framework is conducted to demonstrate how life-cycle cost analysis can be used to help design monitoring solutions by establishing cost/benefit benchmarks for consideration by bridge managers.

Introduction

The challenge of addressing the increasingly urgent need to maintain, repair, and manage ageing civil infrastructure is well documented and widespread across many nations. The issue is of importance as the quality, quantity, and readiness of civil infrastructure directly impacts the economic and social well being of a society (Frangopol and Liu 2007). To address this problem, infrastructure managers urgently need methodologies and technologies to cost-effectively allocate limited budgets that optimally balance lifetime structure performance and life-cycle maintenance costs.

Researchers and engineers around the world have been developing and implementing different management programs to maintain satisfactory infrastructure performance from a long-term economic point of view. One problem facing such programs is that visual inspection-based condition states are often used to determine infrastructure performance. In such approaches, the actual infrastructure safety level is not adequately accounted for and maintenance actions may not be cost effective. For example, it is possible that a structure with satisfactory visual condition states may contain invisible flaws such as the debonding of rebar in a reinforced concrete structure due to corrosion, thus resulting in a serious safety concern. On the contrary, it is also possible that a structure with a poor visual condition state may be structurally sound with only minor repairs needed. In such a case, visual defects may result in unnecessary repair actions and a non-optimal allocation of scarce resources. Another significant problem facing infrastructure managers is that in many cases identified deficiencies are greater than those that can be addressed within available budgets. In such cases, managers must accept solutions that achieve the highest level of performance within budgetary constraints. Conversely, if resources are available, managers have the option to maintain structures at a higher level of performance than previously prescribed for developing the minimum life-cycle cost solution (Frangopol and Liu 2007).

In response to the above concerns, several recent research efforts have focused on management programs that simultaneously consider the performance objectives of condition, safety, and cost for the development of maintenance actions in a life-cycle context. Such methods utilize multi-objective optimization to develop a list of alternative solutions that allow a bridge manager to actively select the most desirable balance between conflicting objectives (Liu and Frangopol 2006). Each solution, termed Pareto optimal, is one such that there does not exist another solution that can improve one objective of the optimized solution without sacrificing at least one of the other objectives. Such management systems provide the flexibility for bridge managers to explore the feasibility of different maintenance actions to satisfy specified requirements within provided budget constraints.

Paramount to the success of any management program is an accurate modeling of the problem and the accuracy of the information fed into that model. This is particularly difficult in a life-cycle analysis due to the amount of uncertainty that must be properly accounted for over the useful lifespan of a structure. In addition to the uncertainties associated with a point-in-time analysis, which include member geometries, material properties, loads and their effects, a life-cycle analysis must consider how each of these change over time due to deterioration, changes in the functionality or use of the structure, or unanticipated load demands. One challenging, yet very promising area of research to help reduce some of these uncertainties and improve the modeling process is the integration of structural health monitoring (SHM) into infrastructure management systems (IMS). Using advanced sensing/information technology and structural modeling/identification schemes, SHM obtains real-time, structure-specific information. SHM applications include structural condition evaluation, parameter identification, model development and updating, and real-time monitoring (Susoy et al, 2007). Although most commonly used to update finite element models (FEM), SHM technologies have the potential to greatly improve existing bridge management systems through more accurately modelling random variable input parameters. This is of benefit because the use and acceptance of reliability-based life-cycle management (LCM) methods is limited by the fact that even after a structure is modeled, slight variations in the input parameters can produce radically different results, thus decreasing the confidence and perceived value of the process (Estes 1997).

Although SHM technologies have the potential to significantly enhance the amount and quality of information utilized in IMS, this information comes with a cost that must be considered in a life-cycle context—the cost of monitoring should include initial design/construction, operational, inspection, repair, and maintenance expenses. As such, it would be expected (unless code driven) that a bridge manager would not employ the use of SHM unless the cost/benefit of the information obtained outweighed the costs of using SHM. As such, it is necessary to develop the metrics for quantifying the costs and benefits associated with monitoring solutions. Furthermore, the design with consideration of different monitoring possibilities then becomes an optimization problem to obtain the most benefit at the least cost.

A change in risk at a point in time or a change in the risk profile over time is a key metric in quantifying the benefit of a monitoring solution. Although the initial and life-cycle costs associated with SHM may be more immediately identified, monitoring has the capacity to reduce life-cycle costs by assisting in correctly scheduling maintenance and inspections, conducting the correct structural repairs when repairs are needed, and by reducing the likelihood of failure. Qualitatively, it is appropriate to associate SHM with the ability to provide warning when critical thresholds are surpassed or to state that a structure is safer with an on-board monitoring system. However, this is unfortunately of limited use to a bridge manager operating in a resource constrained environment unless a dollar amount can be specified. The inclusion of risk in existing management methodologies provides the ability to quantify, assess, and accurately capture the potential cost savings, or utility, associated with SHM.

Risk-Based Decision-Making and Reliability-Based Life-Cycle Management: A Synergistic Approach

The considerations and procedural steps for risk-based decision-making and reliability-based life-cycle management are similar and complimentary in nature as shown in Figure 5.1. They are similar in that both use a probabilistic formulation of a problem to deal with uncertainty. Once modeled, a system is assessed and consequences or benefits of different possible decisions can be evaluated. Once a particular decision is chosen, the model can then be updated and the system reevaluated in terms of consequence, safety, performance, cost, or condition at a future time interval. Both approaches are complimentary in nature as each uses a subset of the other within its framework. For infrastructure management systems, risk-based decision-making often utilizes a reliability analysis to obtain the probability of failure for each outcome within the risk assessment. For reliability life-cycle cost analysis, risk is typically utilized to identify and consider the appropriate life-cycle costs associated with the cost of failure.

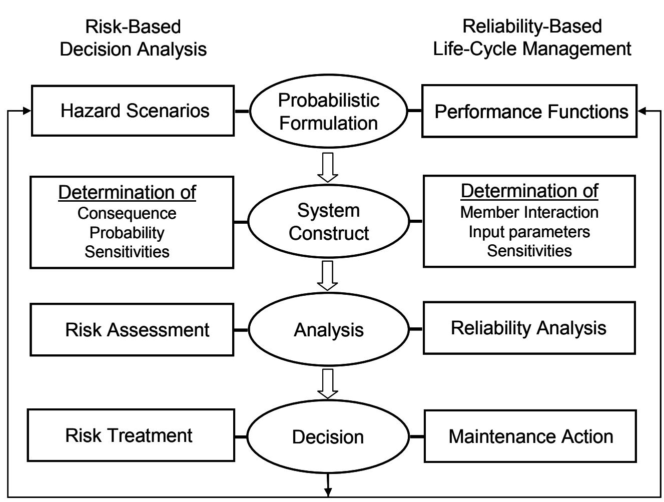

Fig.5.1. Decision-making frameworks

It should be noted that both approaches provide a natural and flexible decision-making methodology in the presence of uncertainty. Using either provides the capability to assess multiple courses of action, allows new information to be introduced into the models, and provides managers the ability to include their preferences or experience. As such, one approach will not supersede the other. Instead, the approaches can be utilized in parallel or the strengths of each can be leveraged in a combined approach.

Quantifying Utility for Monitoring Systems on Bridge Structures

SHM Design Approach

A combined approach that leverages risk-based decision-making and reliability-based life-cycle management is of particular interest in the design and analysis of monitoring systems. In evaluating the cost or benefit of monitoring, two methods are likely. One could first select a monitoring system and subsequently project the costs and estimated benefit in a life-cycle context, or one could first quantify the performance needed from SHM to achieve a utility benchmark and subsequently design a monitoring solution to obtain the required performance. Because identified repair and maintenance needs are currently greater than available budgets to address the problem, it is likely that the adoption of SHM for bridge structures will be incremental in nature. Furthermore, because the actual benefit of any monitoring system will ultimately depend on the actual information collected, the design and initial assessment of such systems must be based on anticipated information, or a pre-posterior analysis. For these reasons, the second approach to the design and assessment of SHM is desirable. By investigating structural models, it is possible to quantify the value of reducing uncertainty through the collection of structure specific information. As such, bridge managers are more likely to view SHM as an investment rather than a sunk cost. Additionally, such an investigation provides focus to the design of a SHM system and helps to answer the questions of what, where, when, and how to monitor. This is of particular interest in a risk-based decision-making approach where one of the main challenges in modeling a complex system is controlling the number of events, or possible outcomes, which can become extremely large.

Quantifying the Costs and Benefits of SHM

The minimum expected life-cycle cost with respect to lifetime performance is the most widely used criterion for design optimization of a new structural system. The general form of the expected life-cycle cost can be calculated as (Frangopol et al. 1997):

$$C_{ET} = C_T + C_{PM} + C_{INS} + C_{REP} + C_F \tag{5-1}$$

where C_{ET} = expected total cost, C_T = initial design/construction cost, C_{PM} = expected cost of routine maintenance, C_{INS} = expect cost of performing inspections, C_{REP} =

expected cost of repairs and C_F = expected cost of failure. Inclusion of monitoring into this general form results in:

$$C_{ET}^0 = C_T^0 + C_{PM}^0 + C_{INS}^0 + C_{REP}^0 + C_F^0 + C_{MON} \quad (5\text{-}2)$$

where C_T^0, C_{PM}^0, C_{INS}^0, C_{REP}^0, C_F^0 have the same meaning as C_T, C_{PM}, C_{INS}, C_{REP}, C_F, respectively, but are associated with the case of monitoring. C_{MON} is the expected cost of monitoring which is:

$$C_{MON} = M_T + M_{OP} + M_{INS} + M_{REP} \quad (5\text{-}3)$$

where M_T = expected initial design/construction cost of the monitoring system, M_{OP} = expected operational cost of the monitoring system, M_{INS} = expected inspection cost of the monitoring system, and M_{REP} = expected repair cost of the monitoring system. The operational cost of the monitoring system would include the cost of power (battery or electricity), as well as the costs associated with data processing and data management. The benefit of the monitoring system, B_{MON}, is then captured through a comparison of the expected life-cycle total cost with and without monitoring by subtracting Eq. 5-2 from Eq. 5-1 (Frangopol and Messervey 2007a):

$$B_{MON} = C_{ET} - C_{ET}^{\ 0} \quad (5\text{-}4)$$

Inclusion and Quantification of Risk

Risk, or the expected cost of failure C_F in the above equations, can be captured as the product of the likelihood of an event, p_f, and the associated consequences in monetary terms, C, given the event occurs as

$$\text{Risk} = \text{R} = \text{C}_\text{F} = \text{p}_\text{f}\text{C} \quad (5\text{-}5)$$

The risk R is typically utilized in risk-based approaches and the cost of failure C_F is typically utilized in LCM methods.

As written, Eq. 5-5 is limited to a point in time analysis. In order to account for the life-cycle costs as noted in Eq. 5-1 to 5-4, a time-dependent reliability analysis must be conducted. One time-dependent reliability approach, the point-in-time approach, calculates the p_f at different points in time as the structure ages. The reliability of the structure can then be expressed in terms of a hazard function *H(t),* which expresses the instantaneous likelihood of failure in a time interval given that failure has not already occurred. A discount rate of money is then assumed, and the net present value

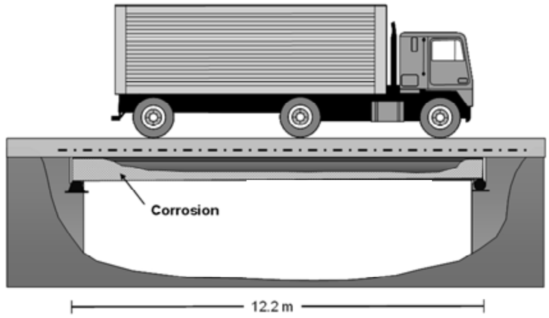

Fig. 5.2. Typical simply supported highway bridge

of the costs detailed in Eq. 5-1 to 5-5 can be calculated for a comparison of monitoring alternatives.

Example Problem

This study builds upon a simple example reported in (Messervey et al. 2006) in which the reliability of a short span, simply supported W690 × 125 steel beam bridge is investigated as the structure ages.

The bridge is subjected to the HS-20 truckload as the steel beams corrode over time. Reliability is calculated with respect to flexure as indicated in the performance function

$$g = f_y S - M_{DL} - M_{LL} \tag{5-6}$$

where f_y is the yield stress, S the section modulus, and M_{DL} and M_{LL} are the dead and live load moment demands, respectively.

Herein, the objective is to quantify the potential benefit of reducing the uncertainty associated with the resistance portion of Eq. 5-6. A sensitivity analysis yields that the uncertainty associated with the resistance is dominated by corrosion induced section loss. Therefore, reducing this uncertainty through the use of SHM is of potential benefit. This potential benefit can be estimated and visualized by repeating a reliability analysis with decremented values of the standard deviation for the section modulus random variable. The result of such an analysis is shown in Figure 5.3. As anticipated, the reliability profile trends higher as more precise information is obtained. The benefit of monitoring increases as the structure ages because the uncertainty associated with the corrosion induced section loss increases as the analysis projects further in time.

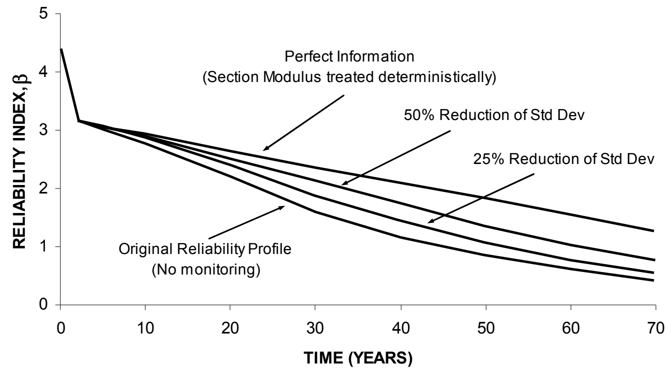

Fig. 5.3. Reliability profile with varying uncertainty associated with the section modulus

Although Figure 5.3 depicts the standard deviation of the section modulus ranging from unchanged (no monitoring) to zero where the section modulus is treated deterministically (perfect information), it is acknowledged that perfect information is unattainable due to the inherent randomness associated with phenomenon itself (aleatory uncertainty) (Ang and de Leon 2005).

To continue, a comparison is made between no monitoring and a monitoring solution that obtains a 50 percent reduction in the standard deviation of the section modulus (a feasible alternative). A minimum required reliability index of 2.0 is established to determine when maintenance actions are required. In this example, the only maintenance action considered is a replacement of the steel beams at a cost of $100,000, which returns the section modulus to its original state and corrosion, is again initiated. The reliability profiles for this scenario are shown in Figure 5.4.

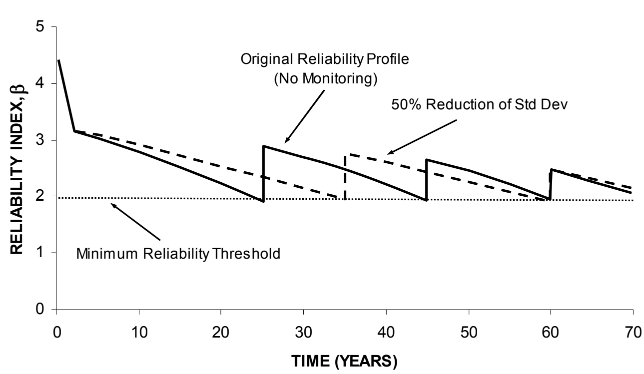

Fig. 5.4. Reliability profile with maintenance actions and a minimum reliability threshold

The life-cycle cost for each option can now be determined to investigate the utility of monitoring. Beginning with the expected costs of repairs, the net present values can be calculated using

$$PV = \frac{FV}{(1+r)^n} \tag{5-7}$$

where FV is the future value at year n and r represents the discount rate of money. Assuming a discount rate of 4% the associated costs of repairs for the two options are

$$C_{REP} = \frac{\$100{,}000}{(1.04)^{25}} + \frac{\$100{,}000}{(1.04)^{45}} + \frac{\$100{,}000}{(1.04)^{60}} = \$64{,}138 \tag{5-8}$$

$$C_{REP}^{0} = \frac{\$100{,}000}{(1.04)^{35}} + \frac{\$100{,}000}{(1.04)^{60}} = \$34{,}848 \tag{5-9}$$

Next, it is desirable to quantify the risk, or cost of failure, associated with each reliability profile. A point in time calculation can be conducted at any specified year as the product of the probability of failure and the consequence of failure. Assuming a consequence of failure of $2,000,000 for clean up, design and reconstruction of a new bridge as well as liability costs, for this example at year 20 the associated costs of failure are

$$C_F(20) = 0.01287 \times 2{,}000{,}000 = \$25{,}747 \tag{5-10}$$

$$C_F^0(20) = 0.00543 \times 2{,}000{,}000 = \$10{,}860 \tag{5-11}$$

However, this same calculation conducted at year 30 would result in the monitoring approach having a higher cost of failure due to the repairs conducted at year 25 for the no monitoring approach as shown in Figure 5.4. This is one reason a point-in-time calculation is not suitable for a life-cycle analysis. A second problem with such an approach is that it fails to account for previous structural performance. A better and more appropriate method is to utilize a hazard function. The conditional probability of failure in time (t, t+dt) given no failure in (0, t) involves the hazard function. This function represents the instantaneous rate of failure given that failure has not already occurred as

$$H(t) = -\frac{dp_s(t)}{dt} \cdot \frac{1}{p_s(t)} = -\frac{S^{'}(t)}{S(t)} \tag{5-12}$$

where $p_s(t)$ is the probability that an element is safe at any time t, which is also referred to as the survivor function $S(t)$. Table 5.1 shows the calculation of the hazard function, or failure rate $H(t)$, and the associated annual risk in dollars for the no monitoring approach for the time period between 20 and 25 years.

Table 5.1. Development of the Hazard Function and Annualized Risk

Yr	Probability of Survival, p_s	Derivative dp_s/dt	Hazard Function, $H(t)$	Annual Risk 2,000,000 $H(t)$
20	0.9871	-	-	-
21	0.9849	-0.0022	0.0022	4478.78
22	0.9824	-0.0025	0.0026	5136.07
23	0.9795	-0.0029	0.0029	5869.38
24	0.9763	-0.0033	0.0033	6684.38
25	0.9726	-0.0037	0.0038	7586.76

Repeating this process for the monitoring approach and expanding the calculations to encompass the entire life cycle being considered, the hazard functions can be created and observed as shown in Figure 5.5.

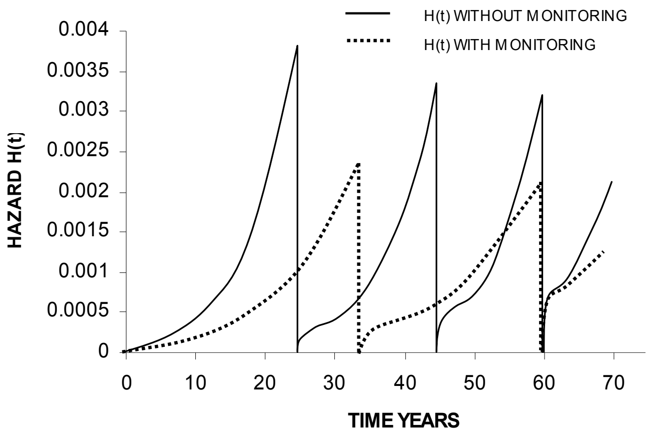

Fig 5.5. Hazard functions with and without monitoring

Eq. 5-7 is then used to calculate the net present value of each annual expected cost of failure (Annual Risk) from Table 5.1. A summation over the life of the structure provides the total expected cost of failure and can be used as a metric to compare the two approaches. In this example these summations result in:

$$C_F = \$44{,}204 \tag{5-13}$$

$$C^{o}_{F} = \$27{,}371 \tag{5-14}$$

Temporarily setting aside the life-cycle costs associated with monitoring as identified in Eq. 5-2 and 5-3, the expected utility B_{MON} of employing SHM can be calculated using Eq. 5-4. For this example, these calculations capture the present value of all expected repair and failure costs for each option and provide the difference as a metric in terms of utility as

$$B_{MON} = (\$64{,}138 + \$44{,}204) - (\$34{,}848 + \$27{,}371) \tag{5-15}$$

$$= \$46{,}123$$

This value can be utilized as a benchmark for the design and consideration of a monitoring system. For a bridge manager, a potential cost savings of \$46,123 is attainable through the collection of more precise information for the section modulus over time. For the engineer designing a monitoring system, it can now be concluded that the system will be cost beneficial as long as the life-cycle cost does not exceed \$46,123 and the system can indeed provide a 50 percent reduction of the section modulus standard deviation over time.

It is important to highlight that this analysis did not account for the fact that the data obtained from monitoring could result in a change of the mean value for the section modulus, which is to say that a particular bridge could perform better or worse than predicted. In addition, this analysis did not account for any reduction in the probability of a sudden catastrophic failure through the notion of critical threshold values of the monitored data. This concept is of value and is left as a topic for future research.

Conclusions

This paper presents an investigation of how to quantify the value of obtaining more precise information in the life-cycle management of structural systems with the motivation of obtaining design benchmarks for structural health monitoring systems. The effect of obtaining more precise information is modeled through the reduction of the standard deviation of random variables within performance functions used to model a structure's performance over time within a reliability analysis. In a probabilistic analysis, more precise information leads to increased structural reliability, decreased risk, and more appropriate maintenance actions which all result in lower life-cycle costs. However, more precise information cannot be obtained without incurring the initial and life-cycle costs of utilizing SHM. Determining if the value of the expected information is worth the cost is similar to pre-posterior analyses often utilized in Bayesian risk-based decision-making. However, the process needs to be appropriately modified for use in a life-cycle context. This paper demonstrates such a procedure and establishes a metric to quantify the potential utility of a monitoring system. This metric can be utilized as a decision-making tool for a bridge manager and can also be utilized as a benchmark in the design of a monitoring solution. The next appropriate steps for the development of this approach are to include more complex maintenance actions, to employ multi-objective optimization, and to expand the concept of utility to include the structure in the context of a larger bridge network.

Acknowledgment

This paper is based on Frangopol, D.M., and Messervey, T. (2007b). The support of the National Science Foundation through grants CMS-0217290 and CMS-0509772 to the University of Colorado, Boulder, and grants CMS-0638728 and CMS-0639428 to Lehigh University are gratefully acknowledged. Also, the support provided by the Collaborative Research Center SFB 477 "Monitoring of Structures" funded at the Technical University of Braunschweig by the German Research Foundation (DFG) is appreciated. The opinions and conclusions presented in this paper are those of the authors and do not necessarily reflect the views of the sponsoring organizations.

Additional Resources

Estes, A. C., and Frangopol, D. M., 2005. "Life-cycle evaluation and condition assessment of structures," Chapter 36 in *Structural Engineering Handbook, 2nd Edition,* W-F. Chen and E. M. Lui, eds., CRC Press, 36-1 to 36-51.

References

Ang, H-S and D. de Leon, 2005. "Reliability-based management of inspection, maintenance and repair of offshore structures," *Structure and Infrastructure Engineering,* Taylor and Francis, 1(1), 19-31.

Estes, A.C. 1997. A System Reliability Approach to the Lifetime Optimization of Inspection and Repair of Highway Bridges. Ph.D. Dissertation, Department of Civil, Environmental and Architectural Engineering, University of Colorado at Boulder.

Estes, A. C., and Frangopol, D. M., 2005. "Life-cycle evaluation and condition assessment of structures," Chapter 36 in *Structural Engineering Handbook, 2nd Edition,* W-F. Chen and E. M. Lui, eds., CRC Press, 36-1 to 36-51.

Frangopol, D.M., Lin, K.Y., and Estes, A.C., 1997. "Life-cycle cost design of deteriorating structures," *Journal of Structural Engineering,* ASCE, 123(10), 1390-1401.

Frangopol, D.M., and Liu, M., 2007. "Maintenance and management of civil infrastructure based on condition, safety, optimization, and life-cycle cost," *Structure and Infrastructure Engineering*, 3(1), 29-41.

Frangopol, D.M., and Messervey, T. B., 2007. "Integrated life-cycle health monitoring, maintenance, management, and cost of civil infrastructure," *Proceedings of the International Symposium on Integrated Life-Cycle Design and Management of Infrastructures*, Tongji University, Shanghai, China, May 16-18 (Keynote Paper); in *International Symposium on Integrated Life-cycle Design and Management of Infrastructure*, Lichu, F., Limin, S., and Zhi, S., eds., Tongji University Press, Shanghai, 2007, 216-218; full 12 page paper on CD-ROM.

Frangopol, D.M., and Messervey, T. (2007); "Risk assessment for bridge decision making," Proceedings of the Fourth Civil Engineering Conference in the Asian Region, CECAR 4, Taipei, Taiwan, June 25-28, 2007 (invited paper), published in ASCE Tutorial and Workshop on Quantitative Risk Assessment, Taipei, Taiwan, June 25-28, 2007, pp. 37-42.

Liu, M., and Frangopol, D.M., 2006. "Optimizing bridge network maintenance management under uncertainty with conflicting criteria: Life-cycle maintenance, failure, and user costs," *Journal of Structural Engineering,* ASCE 132 (11), 1835-1845.

Messervey, T.B., Frangopol, D.M. and Estes, A.C. 2006. “Reliability-based life-cycle bridge management using structural health monitoring,” *Proceedings of the Third International Conference on Bridge Maintenance, Safety, and Management,* IABMAS’06, Porto, Portugal, July 16-19, 2006; in *Bridge Maintenance, Safety, Management, Life-Cycle Performance and Cost*, P.J.S. Cruz, D. M. Frangopol, and L.C.Neves, eds., Taylor and Francis Group plc, London, 545-546, and full paper on CD-ROM, Taylor and Francis Group plc, London, 8 pages on CD-ROM.

Susoy, M., Catbas, F.N., and Frangopol, D.M., 2007. “SHM development using system reliability,” *Proceedings of the Tenth International Conference on Applications of Statistics and Probability in Civil Engineering,* ICASP 10, Tokyo, Japan. July 31-August 3, 2007; in *Applications of Statistics and Probability in Civil Engineering*, Kanda, J., Takada, T., and Furuta, H., eds., Taylor and Francis Group plc, London, 2007, 79-80.

Chapter 6: An All-Hazards Methodology for Critical Asset and Portfolio Risk Analysis

By Bilal M. Ayyub, Ph.D., P.E., and William L. McGill, P.E., Center for Technology and Systems Management, Department of Civil and Environmental Engineering, University of Maryland College Park, MD, USA

Abstract

This paper develops a quantitative all-hazards methodology for critical asset and portfolio risk analysis (CAPRA) that considers both natural and human-caused hazards. A general formula for all-hazards risk analysis is obtained that resembles the traditional model based on the notional product of consequence, vulnerability, and threat, though with clear meanings assigned to each parameter. The methodology is briefly introduced and demonstrated using several illustrative examples based on notional information.

Background

In recent years, decision-makers charged with protecting critical assets have taken an all-hazards approach to risk management by focusing on both natural and human-caused hazards (Waugh 2005), where each individual hazard type is physically unique and presents its own set challenges with its characterization and assessment. However, in contrast to natural hazards that are indiscriminate and without malicious intent, a unique challenge with assessing risks due to the deliberate actions of intelligent human adversaries is their ability to innovate and adapt to a changing environment. Although historical data can be relied upon to estimate annual occurrence rates for natural hazards affecting a region given that the timescale of geological and meteorological change is much greater than the planning horizon for most homeland security decisions, assets in this same region are always plausible targets for adversaries despite a lack of past incidents.

This paper describes a general process for quantitatively assessing risks to critical assets and portfolios considering both natural and human-caused hazards that builds on previously published ideas on security effectiveness assessment, terrorism risk analysis, natural hazards risk analysis, infrastructure risk analysis and interdependency analysis, and systems risk and reliability analysis. The primary objectives of this paper are to present a general equation for all-hazards risk assessment, develop a simple model for portfolio interdependency analysis, and demonstrate the application.

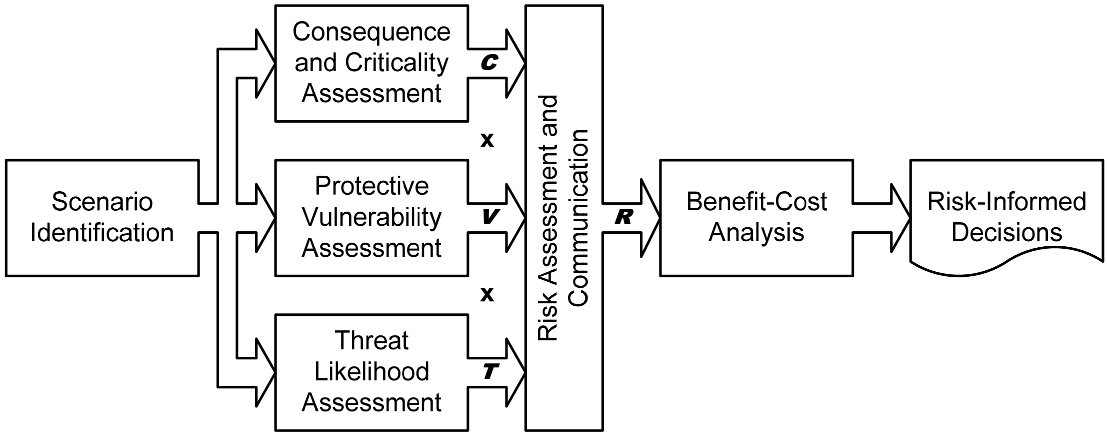

Fig. 6.1. A methodology for critical asset and portfolio risk analysis.

Asset Analysis

A five-phase process for asset level analysis is adopted as shown in Figure 6.1. Since all portfolios, whether defined by a particular function or comprised of otherwise unrelated elements, are defined by their assets, asset level analysis provides the basic information needed to assess risk at higher levels of abstraction. The five steps are based on preliminary work described in Ayyub et al. (2007) and McGill et al. (2007), with slight modification to accommodate new thinking. Each phase is briefly discussed in the following sections.

Scenario Identification

The scenario identification phase constructs an exhaustive set of hazard and threat scenarios that are relevant to a given asset based on its inherent susceptibilities of its key elements to a wide range of natural and human-caused initiating threat events. In the context of the proposed method, a key element is one that contributes directly to one or more missions associated with an asset, and a hazard or threat scenario is the pairing of a specific hazard or threat type with a susceptible key element. Susceptibility is treated as a binary variable, where a value of one indicates the key element can be damaged by a specific hazard or threat type. Once a complete set of hazard and threat scenarios is obtained, selected scenarios can be filtered out from additional analysis either if the rate of occurrence is perceived to be sufficiently low relative to the adverse affects or if the effects are not significant enough to warrant attention.

Consequence and Criticality Assessment

The consequence and criticality assessment phase assesses the loss associated with a given hazard or threat scenario as a function of degree of damage resulting from the damage-inducing mechanisms associated with a hazard or successful attack. The following gives the probability of a specified degree of loss L given adversary success at achieving damage D, $P_{L|D}$, following the occurrence of a hazard or threat scenario:

$$P_{L|D} = (1 - I_I)(1 - I_R) \tag{6-1}$$

where I_I characterizes the intrinsic resistance to loss given damage (one minus the probability of an unmitigated loss of a specified degree), I_R is the effectiveness of response and recovery interventions (measured as one minus the probability of realizing the specified loss L given a level of unmitigated loss), and the summation is taken over all possible values for unmitigated loss. In general, Eq. 6-1 is used to assess the loss for a variety of consequence dimensions, including casualties, economic loss, environmental damage, and recuperation time.

Protective Vulnerability Assessment

With regards to human-caused threats, the protective vulnerability assessment phase assesses the probability of damage for a variety of alternative attack profiles for each threat scenario. An attack profile is the pairing of a specific threat delivery system (such as a vehicle for an explosive attack) with a relevant intrusion path (such as "via main access road"). The effectiveness of measures to detect, delay, respond to, and defeat are considered to arrive at an overall measure of effectiveness, or reliability, of the security or protection apparatus for each attack profile. The probability of damage, P_D, can be obtained as:

$$P_D = (1 - I_S)(1 - I_A)(1 - I_H) \tag{6-2}$$

where I_S is the measure of security system effectiveness or reliability (one minus the probability of adversary success), I_A is the measure of effectiveness for denial interventions (one minus the probability of exposing the target to the threat's damage inducing mechanisms), and I_H is the effectiveness of hardness interventions (one minus the fragility of the target with respect to the intensity of the threat). The model in Eq. 6-2 was developed based on previous work by Martz and Johnson (1987), Dessent (1987), and Hicks et al. (1999). For natural hazards, $P_D = (1 - I_H)$.

Threat Likelihood Assessment

For human-caused threats, the threat likelihood assessment phase estimates the annual rate of occurrence for each attack profile based on the perceived attractiveness of each the asset, threat scenarios, and attack profiles. Assuming rational adversaries (Hoffman 1998) that seek to maximize expected utility with respect to their own perceptions of risk and reward (Pate-Cornell and Guikema 2002), the relative attractiveness, A_P, of an attack profile can be obtained as:

$$A_P = P_{VP}U_P \,/\, \Sigma\, P_{VP}U_P \tag{6-3}$$

where P_{VP} is the probability that the profile (intrusion path) is visible to the adversary, U_P is the expected utility of an attack profile as perceived by the adversary, and the summation in the denominator of Eq. 6-3 is taken over all attack profiles. This model basically assumes that the probability of attack for a given attack profile is proportional to its attractiveness, and can be thus called the proportional attractiveness method. The choice of utility model for the adversary depends on the specific preferences, motivations, risk attitudes, and such. Yager (2007) suggests multiple prototypical adversaries be considered, including those that seek to maximize potential gain, maximize probability of success, or maximize return on investment. Moreover, if one conservatively assumes that the adversary has perfect knowledge of consequences and vulnerabilities, the parameters used to estimate utility based on gain and probability of success can be pegged to defender information obtained during the consequence and criticality assessment and protective vulnerability assessment phases.

Analogous to profile attractiveness, estimates of scenario attractiveness and asset attractiveness can be obtained as

$$A_S = P_{VS}U_S \,/\, \Sigma\, P_{VS}U_S \qquad (6\text{-}4)$$

$$A_A = P_{VA}U_A \,/\, \Sigma\, P_{VA}U_A \qquad (6\text{-}5)$$

where U_S can be taken as the maximum utility among all attack profiles associated with a given threat scenario (or some other functional), and U_A is the maximum utility among all threat scenarios associated with a given asset (or some other functional). The summation in the denominators of Eq. 6-4 and 6-5 are taken over all threat scenarios and assets, respectively. This model assumes that the overall utility for a scenario (asset) is completely a function of the utilities assigned to the associated attack profiles (scenarios).

The annual rate of occurrence, λ, for an attack profile can be obtained as

$$\lambda = \lambda_0 A_A A_S A_P \qquad (6\text{-}6)$$

where λ_0 is an estimated baseline annual rate of occurrence for a given hazard or threat type. The asset attractiveness, threat scenario attractiveness, and attack profile attractiveness are taken to be surrogates for the probability of attack at a given asset with a given threat type, probability of realizing a certain threat scenario given attack, and the probability of the attack via a certain attack profile given a threat scenario. For natural hazards, the annual rate of occurrence is simply the estimated frequency of occurrence from past data and expert opinion.

Risk Assessment

From Eq. 6-1, 6-2, and 6-6, the total annual risk expressed as the probability distribution over a continuum of losses L for an asset with respect to a given threat type can be expressed as

$$P_L = \sum_S \sum_P (1 - I_R)(1 - I_I)(1 - I_H)(1 - I_A)(1 - I_S) A_P A_S A_A \tag{6-7}$$

where the summations are taken over all threat scenarios S and associated attack profiles P.

In an effort to provide actionable risk information to decision-makers, the risk results determined from Eq. 6-7 should be accompanied by knowledge of how sensitive these results are to small favorable changes in each of the model parameters. Actionable risk assessments not only communicate risk but also offer guidance on what aspects of risk contribute most to the problem. Such information can be used to guide decision-makers toward cost-effect risk mitigation solutions. A simple formula for the relative sensitivity, S, of risk to changes in each model parameter is given as

$$S = (\Delta_p R/R)/p \tag{6-8}$$

where $\Delta_p R$ is the change in risk due to a favorable fractional change, p, in a given model parameter. The percentage p appears in the denominator in Eq. 6-9 so that the relative sensitivity S communicates how much of an improvement is realized relative to improvement in the model parameters (for example, $S = 4$ means a 1 percent favorable change in a model parameter resulting in a 4 percent reduction in risk). For example, the sensitivity of risk to security system effectiveness would look at how risk changes due to, say, a favorable 1 percent ($p = 0.01$) change in the value for this parameter (in the directed toward 1). Again, knowledge of the risk obtained from Eq. 6-7 in conjunction with the sensitivities from Eq. 6-8 provides guidance to decision-makers on which variables offer the greatest potential for cost-effective risk reduction.

Benefit-Cost Analysis

Benefit-cost analysis determines the cost-effectiveness of proposed countermeasures and consequence mitigation strategies for reducing the risk associated with an asset or portfolio of assets. The benefit-to-cost ratio for a given investment alternative can be calculated as (Ayyub 2003):

$$\text{Benefit-to-Cost Ratio} = B / C \tag{6-9}$$

where the benefit B is the difference between the risk before and after implementation, and the cost C is the equivalent annual cost to implement and sustain the risk mitigation action over a specified time horizon. The probability that a target benefit-to-cost ratio, α, will be realized can be determined as (Ayyub 2003)

$$\Pr(B/C > \alpha) = 1 - \Pr(B - \alpha C \leq 0) \tag{6-10}$$

Portfolio Analysis

The overall process for portfolio level risk assessment is similar to the asset level analysis described in the previous section and shown in Figure 6.1, the main differences being that multiple assets are considered according to the definition of the portfolio and that all losses are assessed from a portfolio perspective. In the context of the proposed method, a portfolio is a set or collection of assets of similar attributes, such as membership in a geographic region, jurisdiction, or infrastructure sector.

The primary difference between asset- and portfolio-level risk analysis concerns the assessment of loss. Whereas asset-level analysis estimates loss with respect to the asset, in general portfolio-level analysis considers both direct asset losses and indirect portfolio or system losses arising from physical geographic, cyber, and logical interdependencies. Furthermore, interdependencies can be internal to the portfolio, or arise from external interactions between portfolio assets at the external world.

The expression for total portfolio economic loss, L_P, for a given hazard or threat can be written as

$$L_P = L_D + L_I \tag{6-11}$$

where L_D is the direct economic loss (or aggregate loss as appropriate) to the asset calculated from Eq. 6-1 assessed from the perspective of the decision-maker charged with protecting the portfolio, and L_I gives the loss due to interdependency effects. A simple model for estimating the loss due to interdependency effects can be expressed as

$$L_I = (\mathrm{c}^T \mathrm{K} \mathrm{u}) L_T \tag{6-12}$$

where L_T is the time to recuperate lost function following the occurrence a hazard or threat scenario, c is a vector that assigns a cost per unit time of disruption for each asset in a given portfolio, K is the portfolio interdependency matrix where elements k_{ij} given the percentage degree of disruption to an asset i due to complete loss of asset j ($k_{ij} = 0$ for $i = j$), and u is a disruption vector whose elements corresponds to the degree of disruption of an attacked asset. Note that the model in Eq. 6-12 considers only first-order interdependencies, assumes proportional interdependency relationships between assets, neglects substitution, and assumes a proportional relationship between economic loss and degree of disruption per unit time.

Illustrative Examples

High-Level Asset Analysis

This example demonstrates a high-level application of the proposed methodology to assess the economic risks to an asset with respect to a full suite of natural and man-made hazards. More details on asset-level examples can be found in the papers by Ayyub et al. (2007) and McGill et al. (2007). Note that notional results are used. This example directly assesses values for each of the parameters in Eq. 6-10, such as would be the case if limited resources were available for analysis and data was available primarily in the form of expert judgment. Table 6.1 provides an assessment of each parameter and associated coefficient of variation in parentheses. Table 6.2 gives the contribution to total annual risk from each hazard scenario and the overall sensitivity of risk to a 1 percent fractional favorable change in the vulnerability (Note that coefficients of variation are given in parentheses adjacent to the mean values). From these results, the total annual risk is 10.4 with a coefficient of variation of 0.22, and improvements in the vulnerability of the region to tornados should be targeted for cost-effective risk reduction. Moreover, the results from this analysis can be used to construct a family of loss-exceedance curves such as those shown for mean exceedance rate in Figure 6.2 (Ayyub 2003).

Table 6.1. Parameter Values for Risk Assessment

Hazard / Threat	Maximum Credible Loss (Millions of Dollars)	Vulnerability	Annual Rate of Occurrence
Hurricane	100	0.2 (0.25)	0.2 (0.2)
Tornado	10	0.3 (0.25)	2 (0.2)
Drought	1	0.2 (0.25)	0.1 (0.2)
Winter Storm	10	0.01 (0.25)	3 (0.2)
Nuclear Attack	500	0.8 (0.25)	1E-06 (0.3)
Explosive Attack	3	0.3 (0.25)	0.05 (0.3)
Airplane as Projectile	0.5	0.1 (0.25)	0.01 (0.3)
Biological Attack	100	0.2 (0.25)	1E-04 (0.3)
Industrial Accident	2.5	0.01 (0.25)	0.2 (0.3)

Table 6.2. Risk Assessment Results

Hazard / Threat	Economic Risk (Millions of Dollars per Year)	Sensitivity to Changes in Vulnerability
Hurricane	4 (0.32)	0.39
Tornado	6 (0.32)	0.58
Drought	0.02 (0.32)	0.002
Winter Storm	0.3 (0.32)	0.03
Nuclear Attack	0.0004 (0.39)	3.9E-5
Explosive Attack	0.045 (0.39)	0.004
Airplane as Projectile	0.0005 (0.39)	4.8E-5
Biological Attack	0.002 (0.39)	1.9E-4
Industrial Accident	0.005 (0.39)	4.8E-4

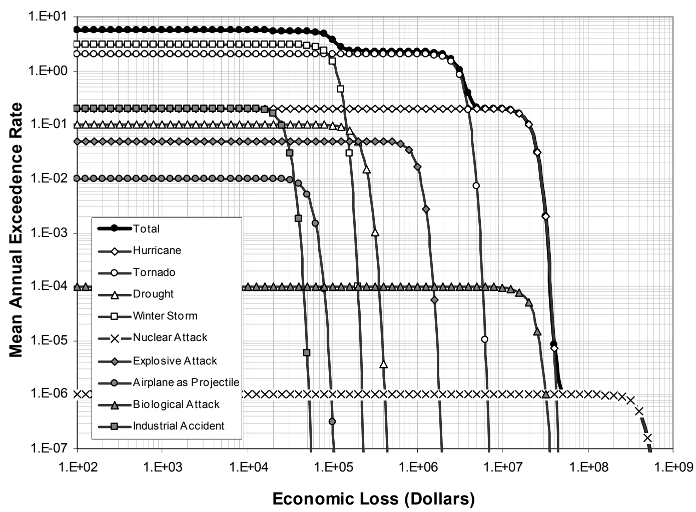

Fig. 6.2. Loss-exceedance curves for the asset-level example

Threat Assessment

This example demonstrates how the discussed approach to threat assessment captures adversary tendencies to shift preferences in response to changes in the security environment. Consider a set of attack profiles for an exhaustive set of two explosive threat scenarios (one against a chemical tank, another against an office building) with conditional casualty risks ($U_P = P_D\mu_L$, where μ_L is the expected loss to the defender / gain to the adversary) and relative attack profile and scenario attractiveness (from Eq. 6-3 and 6-4) as shown in Table 6.3. Values for attack profile attractiveness were determined based on the assumption of perfect visibility and perfect adversary knowledge of key elements and intrusion paths. For simplicity, assume $\lambda_A = \lambda_0 A_A = 1$; when used to obtain total annual risk, this assumption yields the total risk given the occurrence of an explosive attack on the asset. From the information in Table 6.3, the expected total risk given an explosive attack at the asset is about 290 fatalities.

Now consider the implementation of security measures that significantly decrease the probability of adversary success for attack profiles via the access road as described in

Table 6.4. The expected total risk following implementation of these security measures without considering any adjustment in adversary preferences is about 101 fatalities, yielding a reduction in risk of 189 fatalities. With consideration of shifting adversary preferences, the expected total risk following implementation is 131 fatalities, yielding a reduction in risk of 159 fatalities. Thus, according to the proposed model for threat likelihood assessment that captures adversary behavior for this example, the net benefit due to implementation of security measures is less than what would be determined without accounting for shifting adversary preferences.

Table 6.3. Asset Threat Assessment Before Implementation of Security Improvements

Threat Scenario	Attack Profile	Conditional Risk (fatalities)	Relative Profile Attractiveness	Relative Scenario Attractiveness
Explosive attack against chemical tank	Hand emplaced via main gate	10	0.06	0.18
	Hand emplaced via access road	20	0.12	
	Vehicle bomb via main gate	40	0.24	
	Vehicle bomb via access road	100	0.59	
Explosive attack against building	Hand emplaced via main gate	25	0.03	0.82
	Hand emplaced via access road	50	0.07	
	Vehicle bomb via main gate	200	0.28	
	Vehicle bomb via access road	450	0.62	

Table 6.4. Asset Threat Assessment After Implementation of Security Improvements

Threat Scenario	Attack Profile	Conditional Risk (fatalities)	Relative Profile Attractiveness	Relative Scenario Attractiveness
Explosive attack against chemical tank	Hand emplaced via main gate	10	0.13	0.17
	Hand emplaced via access road	5	0.07	
	Vehicle bomb via main gate	40	0.53	
	Vehicle bomb via access road	20	0.27	
Explosive attack against building	Hand emplaced via main gate	25	0.07	0.83
	Hand emplaced via access road	10	0.03	
	Vehicle bomb via main gate	200	0.60	
	Vehicle bomb via access road	100	0.30	

Portfolio Interdependency Analysis

This example illustrates the assessment of interdependency losses associated with portfolio level consequence and criticality assessment. Consider a portfolio of three assets—Asset X, Asset Y, and Asset Z—with interdependency matrix K and loss vector c shown in Table 6.5. Furthermore, consider a single-hazard type affecting this portfolio, and assume point estimates for the degree of functional degradation and recuperation time for each asset following each hazard event (hazard afflicting an asset) are given in Table 6.6. From Eq. 6-12 and the data from Tables 6.5 and 6.6, the total interdependency loss for each hazard event was calculated as shown in last column of Table 6.6.

Table 6.5. Portfolio Interdependency Matrix and Daily Cost of Disruption

Asset	Percent Disruption due to Loss of Asset			Cost per Day of Disruption (Dollars)
	X	Y	Z	
X	NA	0.8	0.3	3,750,000
Y	0.4	NA	0.6	2,500,000
Z	0.9	0.3	NA	1,250,000

Table 6.6. Resulting Interdependency-Related Loss

Asset	Service Disruption (%/Event)	Recuperation Time (Days/Event)	Interdependency Loss (Dollars/Event)
X	0.6	3	3,825,000
Y	0.2	5	3,375,000
Z	0.5	7	9,187,500

Conclusions

This paper described a quantitative all-hazards framework for critical asset and portfolio risk analysis (CAPRA). The data requirements for CAPRA include both historical information and expert opinions, and uncertainty is accommodated as appropriate using standard techniques for uncertainty propagation and representation (Ayyub and Klir 2006). Recent work suggests data from previous risk and vulnerability assessments, assessments of similar facilities or regions, and expert opinion to construct parameter distributions can be aggregated using evidence theory-based techniques (McGill and Ayyub 2007). Future work will seek to demonstrate that the CAPRA framework can effectively capture and propagate uncertainty in a variety of practical forms.

Acknowledgements

Funding for this work was provided by the Maryland Emergency Management Agency (MEMA). The authors wish to thank MEMA and its representatives including Daniel Green, Mel Blizzard, Adam Trister, Christopher Geldart, and Michael Beland for their support.

References

Ayyub, B. M. (2003), Risk Analysis in Engineering and Economics, Chapman & Hall/CRC Press, FL.

Ayyub, B. M., and Klir, G. J. (2006). Uncertainty Modeling and Analysis in Engineering and the Sciences, Chapman & Hall/CRC Press, FL.

Ayyub, B. M., McGill, W. L., and Klir, G. J. (2007). "Critical Asset and Portfolio Risk Analysis for Homeland Security: An All-Hazards Framework." Risk Analysis, In press.

Dessent, G. H. (1987). "Prison Perimeter Cost Effectiveness," Journal of the Operational Research Society, Vol. 10, pp. 975-980.

Hicks, M. J., Snell, M. S., Sandoval, J. S., and Potter, C. S. (1999), "Physical Protection Systems – Cost and Performance Analysis: A Case Study," IEEE AES Systems Magazine, April 1999.

Hoffman, B. (1998). Inside Terrorism, Columbia University Press, NY.

Martz, H. F., and Johnson, M. E. (1987). "Risk Analysis of Terrorist Attacks," Risk Analysis, Vol. 7, No. 1, pp. 35-47.

McGill, W. L., and Ayyub, B. M. (2007). "A Transferable Belief Model for Estimating Parameter Distributions in Structural Reliability Assessment." Computers & Structures, In press.

McGill, W. L., Ayyub, B. M., and Kaminskiy, M. (2007). "Risk Analysis for Critical Asset Protection." Risk Analysis, In press.

Pate-Cornell, M., and Guikema, S. (2002). "Probabilistic Modeling of Terrorist Threats: A Systems Analysis Approach to Setting Priorities Among Countermeasures." Military Operations Research, 7(4), 5-23.

Waugh, W. L. (2005). "Terrorism and the All-Hazards Model." Journal of Emergency Management, 3(2), 8-10.

Yager, R. R. (2007). "OWA Trees and Their Role in Security Modeling Using Attack Trees." Information Sciences, 176(2), 2933-2959.

Chapter 7: A Methodology for the Risk Analysis and Management of Protected Hurricane-Prone Regions

By Bilal M. Ayyub, Ph.D., P.E., Professor and Director, Center for Technology and Systems Management, Department of Civil and Environmental Engineering, University of Maryland

Abstract

This paper introduces a quantitative risk analysis methodology for hurricane prone areas protected by a hurricane protection system. The methodology is intended to assist decision and policy makers and has the characteristics of being analytic, quantitative, and probabilistic. The hazard is quantified using a probabilistic framework to obtain hazard profiles as elevation-exceedance rates, and the risk is quantified in the form of loss-exceedance rates that are based on a spectrum of hurricanes determined using a joint probability distribution of the parameters that define hurricane intensity. The proposed methodology will enable decision makers to evaluate alternatives for managing risk, such as providing increased hurricane protection, increasing evacuation effectiveness, changing land-use policy, enhancing hurricane protection system operations, and enhancing preparedness.

Risk Analysis Methodology

In the engineering community, risk is generally defined as the potential of losses for a system resulting from an uncertain exposure to a hazard or as a result of an uncertain event (Ayyub 2003). Risk should be based on identified risk events or event scenarios. Risk is quantified as the rate (measured in events per unit time, such as a year) that lives, economic, environmental, and social/cultural losses will occur due to the non-performance of an engineered system or component. The non-performance of the system or component can be quantified as the probability that specific loads (or demands) exceed respective strengths (or capacities) causing the system or component to fail, and losses are defined as the adverse impacts of that failure if it occurs. Risk can be viewed to be a multi-dimensional quantity that includes event-occurrence rate (or probability), event-occurrence consequences, consequence significance, and the population at risk; however, it is commonly measured as a pair of the rate (or probability) of occurrence of an event, and the outcomes or consequences associated with the event's occurrence that account for system weakness, that is, vulnerabilities. Another common representation of risk is in the form of an exceedance rate (or probability) function of consequences. In a simplified notional (or Cartesian) product, it is commonly expressed as

$$\text{Risk} = \text{Event rate} \times \text{Vulnerability} \times \text{Consequences} \tag{7-1}$$

This equation not only defines risk but also offers strategies to control or manage risk by making the system more reliable through vulnerability reduction or by reducing the potential losses resulting from a failure. The probability of failure part of the equation can be influenced by engineers by strengthening of existing structures or by adding additional protection; however, the consequence part is highly dependent upon the actions and decisions made by residents, government, and local officials, including first-response and evacuation plans and practices. In densely populated areas, simply increasing the reliability of a hurricane protection system may not reduce risks to acceptable levels and increasing consequences through continued flood plain development can offset any risk reductions.

Risk Analysis Methodology

Probabilistic risk analysis as described by Ayyub (2003), Kumamoto and Henley (1996), and Modarres et al. (1999) was used to develop the overall risk analysis methodology of a protected hurricane-prone region as presented in Figure 7.1. Subsequent sections describe individual parts of the methodology.

Risk associated with a hurricane protection system (HPS) is quantified through a regional hurricane rate (λ) and the probability $P(C > c)$ with which a consequence measure (C) exceeds different levels (c). The loss-exceedance probability per event is evaluated as

$$P(C > c) = \sum_i \sum_j P(h_i) P(S_j \mid h_i) P(C > c \mid h_i, S_j) \tag{7-2}$$

An annual loss-exceedance rate can be estimated as follows.

$$\lambda(C > c) = \sum_i \sum_j \lambda P(h_i) P(S_j \mid h_i) \times P(C > c \mid h_i, S_j) \tag{7-3}$$

where $P(h_i)$ is the probability of hurricane events of type i, $P(S_j|h_i)$ is the probability that the system is left in state j from the occurrence of h_i, and $P(C>c|h_i,S_j)$ is the probability that the consequence C exceeds c under (h_i,S_j). Summation is over all hurricane types i and all system states j in a suitable discretization. Simulation studies of hurricanes for risk analysis require the use of representative combinations of hurricane parameters and their respective probabilities. The outcome of this process is a set of hurricane simulation cases and their respective conditional rates $\lambda P(h_i)$.

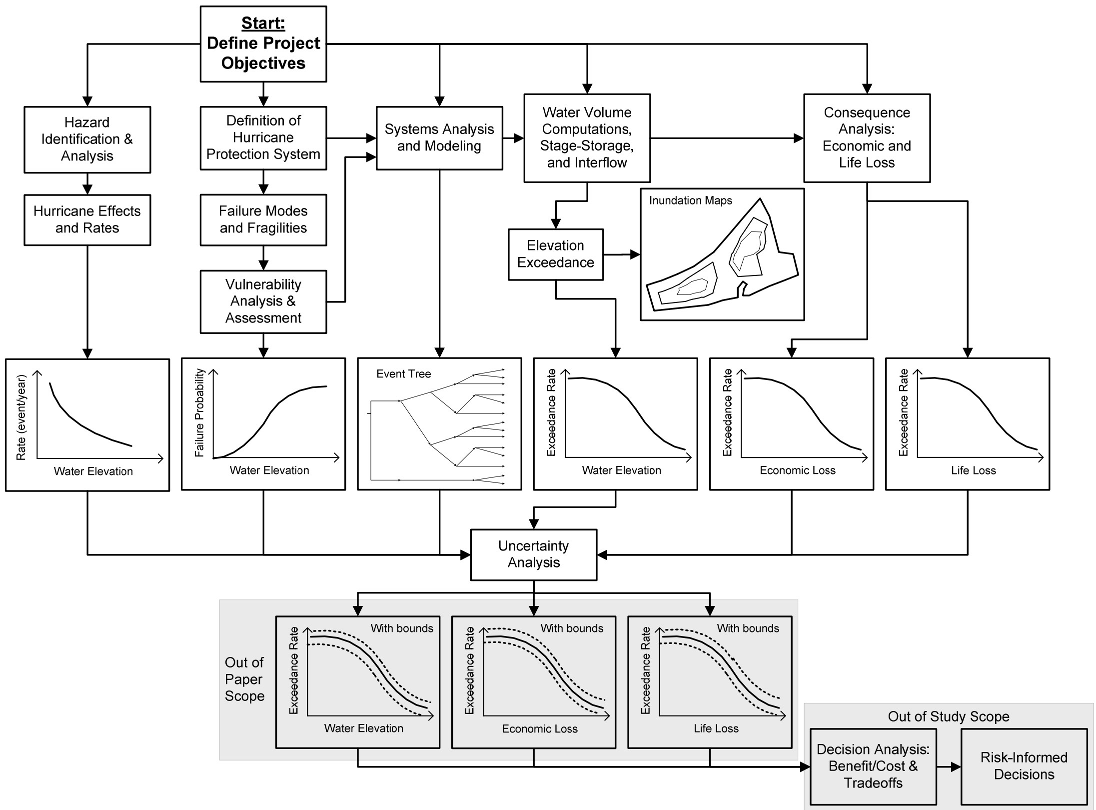

Fig. 7.1. A Methodology for hurricane protection systems.

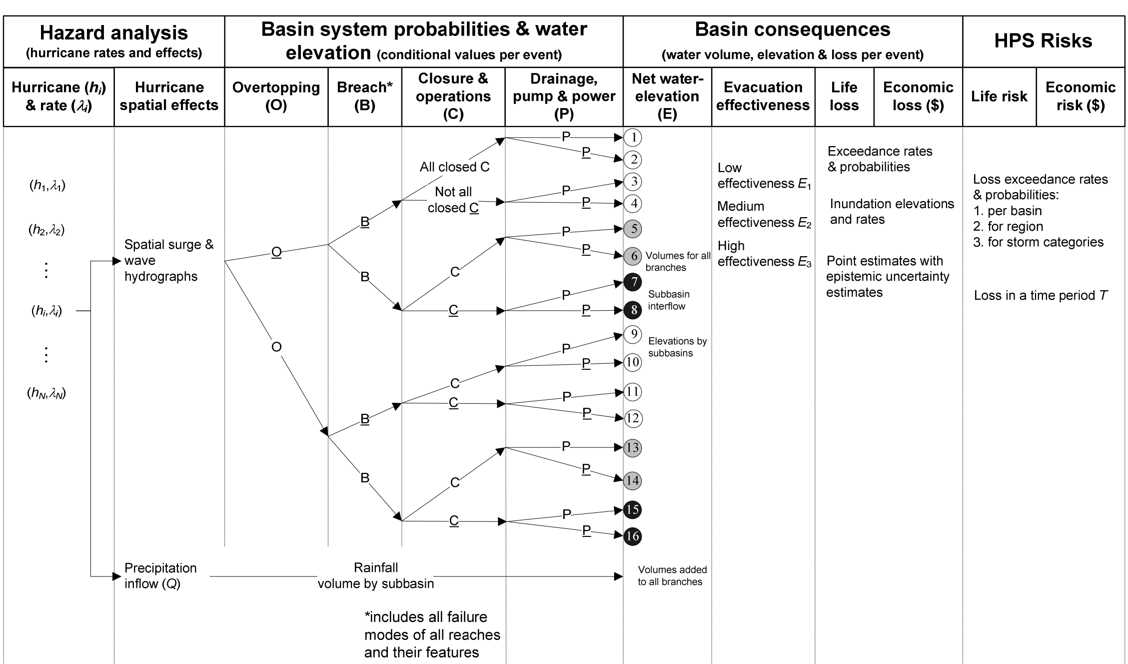

Fig. 7.2. A probability and risk tree for a protected hurricane-prone region.

Evaluation of the regional hurricane rate λ and the probability $P(h_i)$, the conditional probabilities $P(S_j|h_i)$, and the conditional probabilities $P(C>c|h_i,S_j)$ is the main objective of the hurricane model, the system model, and the consequence model, respectively. The probability $P(S_j|h_i)$ covers the states of the components of the HPS, such as closure structure and operations, precipitation levels, electric power availability, failures modes of levees and floodwalls, and pumping station reliability. To assess the state of the HPS given a hurricane event requires an evaluation of the reliability of individual structures, systems and components (for example, levees, floodwalls, pump systems) when they are exposed to the loads and effects of the hurricane (for example, the peak surge, wave action) and the relationship of these elements to the overall function of the system to prevent flooding in protected areas.

The probability and risk tree of Figure 7.2 was based on an influence diagram that is not provided in the paper and simplified to determine the rate of flooding elevations and displaying the results as inundation contours within the basins (see USACE 2006). The processes of transforming inundation to consequences is simplified by grouping communication, warning decision and public execution into an exposure factor parameter applied to lives and property at risk, and grouping power and pumping availability into one event. The events of the tree are defined in Table 7.1.

Risk Quantification

The hurricane protection system was defined in terms of reaches as illustrated in Figure 7.3. Surge and wave hydrographs were simulated using a set of storms representative of all storms with associated rates. Example surge and wave hydrographs are provided in Figure 7.4.

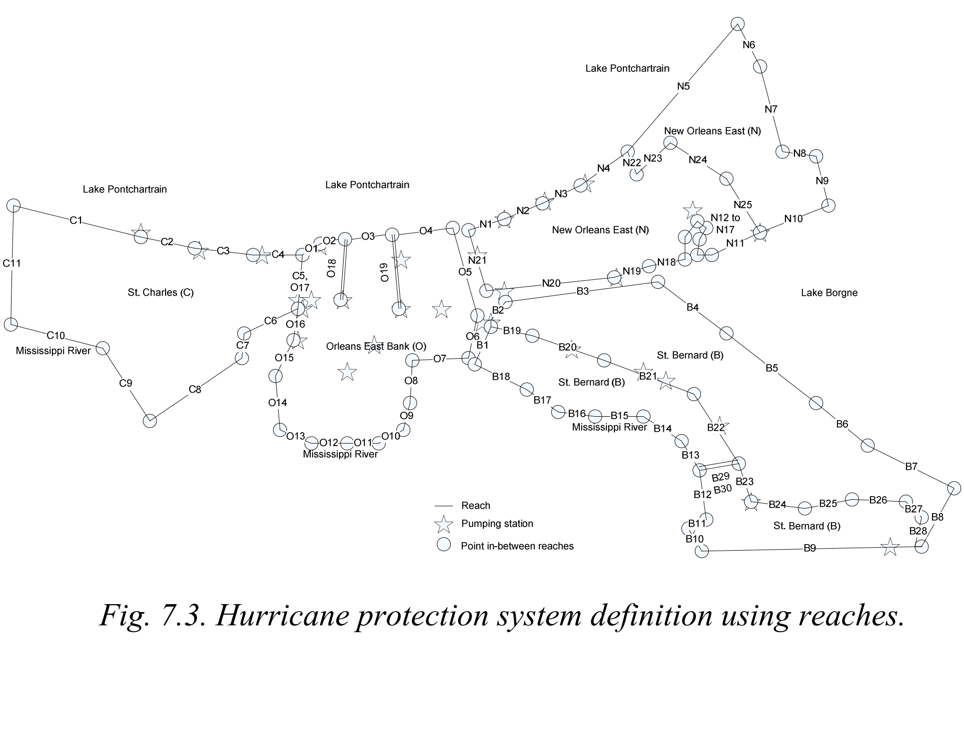

Fig. 7.3. Hurricane protection system definition using reaches.

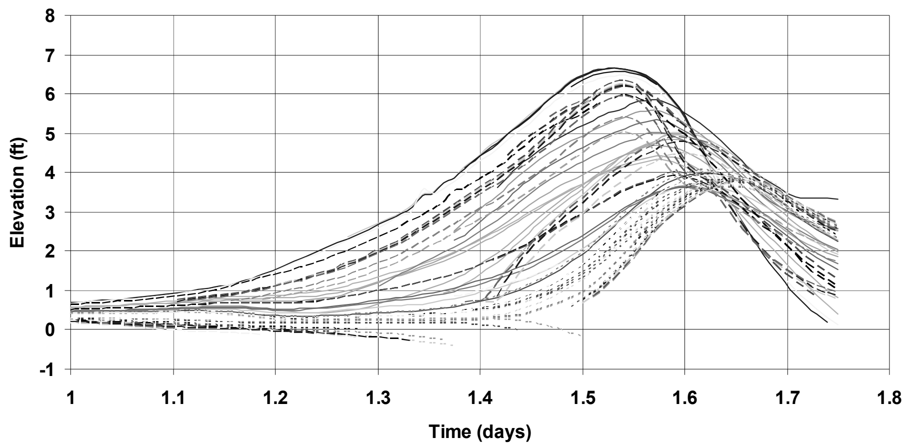

Fig. 7.4. Surge and wave hydrographs.

Table 7.1. Summary of the Event Tree Top Events

Top Event	Description
Hurricane initiating event	The hurricane initiating event is mapping of hydrographs of the peak flood surge with waves in the study area with a hurricane rate λ. This event was denoted, $h_i(x,y)$, and has a probability of occurrence, $P(h_i(x,y))$ and a rate of occurrence of $\lambda P(h_i(x,y))$.
Closure structure and operations (C)	This event models whether the hurricane protection system closures, i.e., gates, have been sealed prior to the hurricane. This event depends on a number of factors as illustrated in the influence diagram of Figure 7.3. The closure structures are treated in groups in terms of probability of being closed in preparation for the arrival of a hurricane. This event was used to account for variations in local practices and effectiveness relating to closures and their operations.
Precipitation inflow (Q)	This event corresponds to the rainfall that occurs during a hurricane event. The precipitation inflow per subbasin is treated as a random variable.
Drainage, pumping and power (P)	This event models the availability of power (normal) power for the pump systems. This event is modeled in the event tree to represent a common mode of failure for the pump systems, and is included in developing a model for drainage and pumping efficiency or lack thereof including backflow through pumps. The event also models the availability of the pump system and its ability to handle a particular floodwater volume. This event is treated in aggregate with drainage effectiveness and power reliability including backflow through pumps.
Overtopping (O)	This event models the failure of the enclosure/protection system due to overtopping, given that failure has not occurred by some other (non-overtopping) failure mode. If failure (breach) does not occur, flooding due to overtopping could still result.
Breach (B)	This event models the failure of the enclosure/protection system (e.g., levees/floodwalls, closures) during the hurricane, exclusive of overtopping failures). This event includes all other failures and it models all 'independent' levee/floodwall sections. This event is treated using conditional probabilities as provided in Figure 7.6.

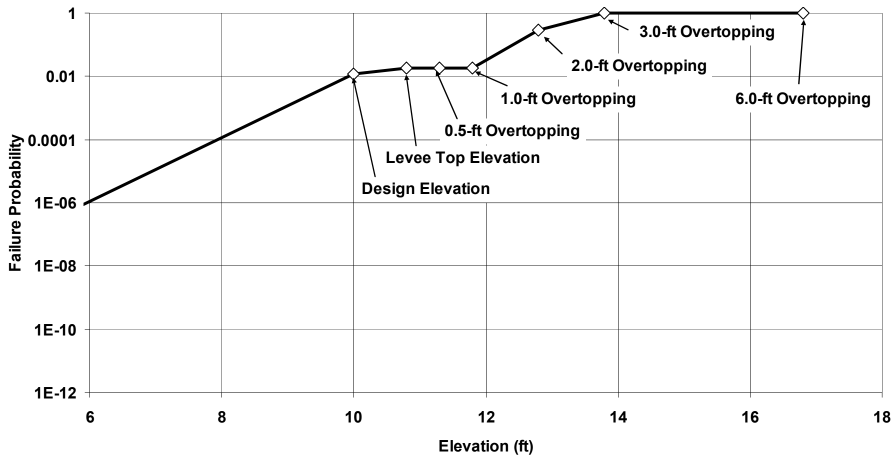

Fig. 7.5. An example fragility curve for a reach or transition

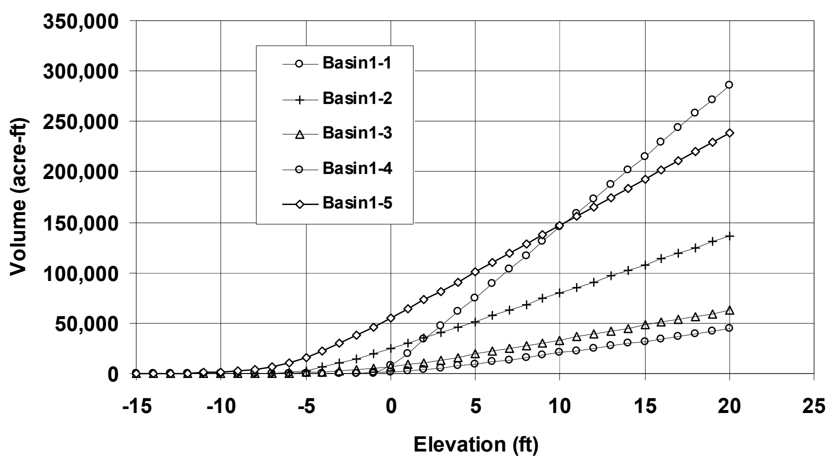

Fig. 7.6. Stage storage for subbasins (1 acre-ft = 43,560 ft^3)

Fragility curves were used for all the reaches and transitions as illustrated in Figure 7.5. Overtopping, gate, and breach water volumes were computed using the Weir equation from hydraulic engineering (Daugherty et al. 1985). Water volumes were added to rainfall water volumes and pumping effects were accounted for to produce net water volumes. These water volumes were used in each subbasin to computer water elevation based on respective stage-storage relationships for the subbasins as illustrated in Figure 7.6.

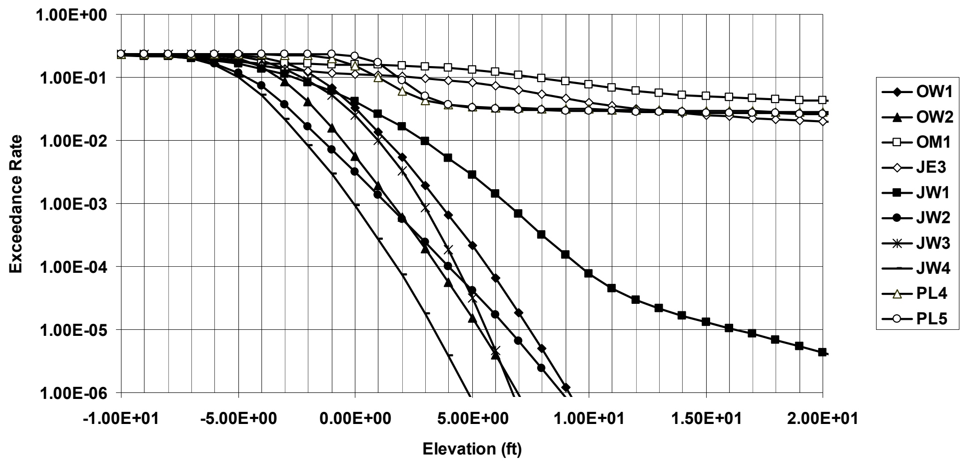

Fig. 7.7. An example elevation exceedance profile

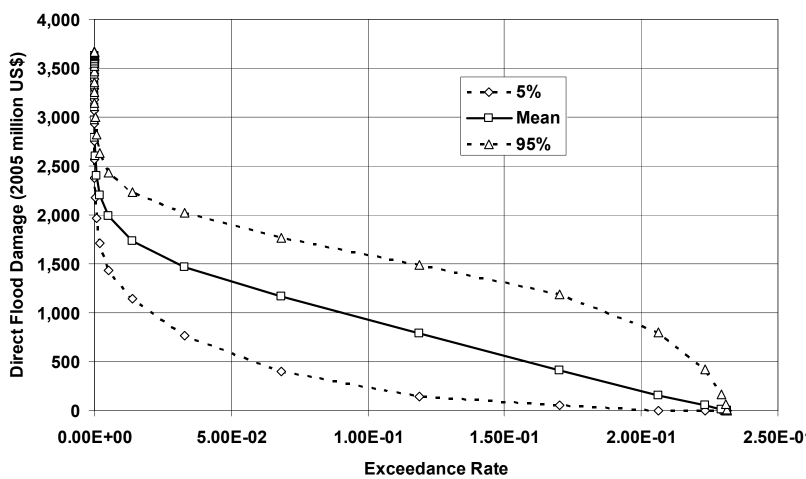

Fig. 7.8. An example economic loss profile

Interflow logic was used to determine final water elevation in each subbasin and compute hazard profiles as elevation-exceedance curves. Figure 7.7 illustrates such a curve. These curves were then combined with loss-elevation curves to produce loss-exceedance curves as illustrated in Figures 7.8 and 7.9. Figure 7.10 shows an example inundation map that can be produced from Figure 7.7.

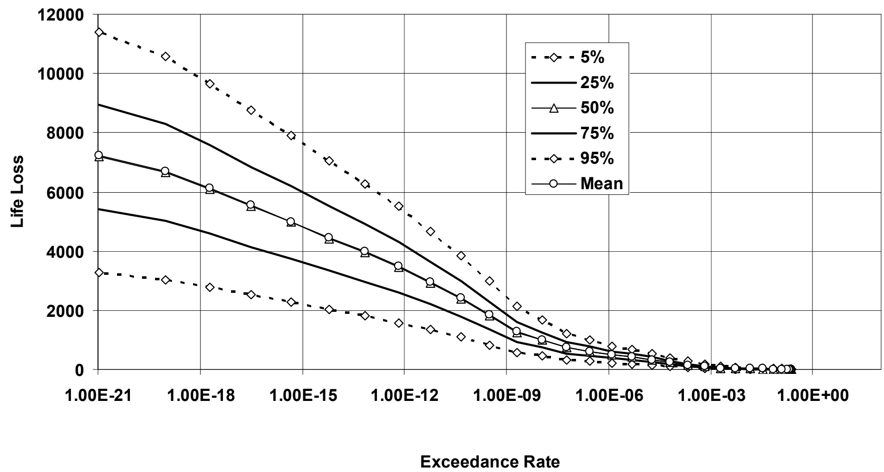

Fig. 7.9. An example life loss profile

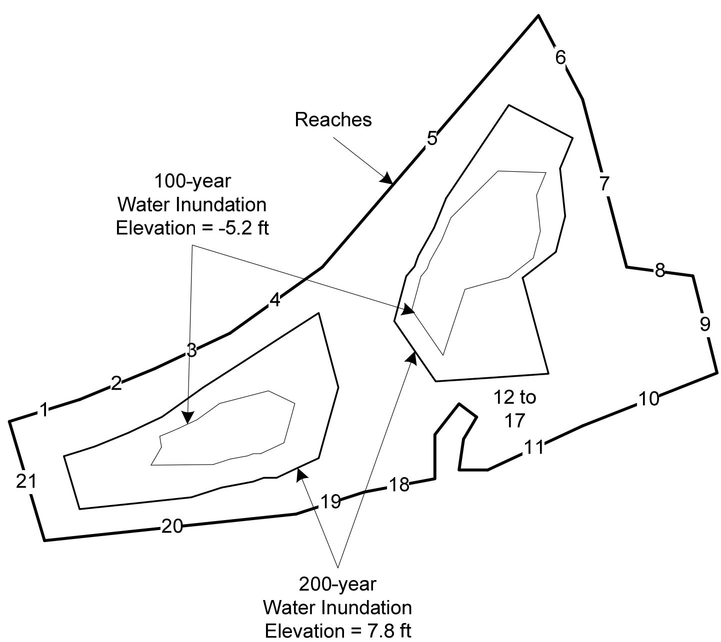

Fig. 7.10. An example inundation map

Benefit-Cost Analysis

Given baseline risk information for an HPS, benefit-cost analysis can be used to assess the cost-effectiveness of alternative risk mitigation strategies. In the context of protecting a region against floods resulting from post-hurricane surges, risk mitigation options include strengthening levees, increasing the span and depth of the levees, relocating residential and commercial centers, and enhancing emergency response procedures. The benefit of a risk mitigation action is the difference between the total annual risk before and after its implementation (Ayyub 2003). The benefit-to-cost ratio is given by

$$\text{Benefit-to-Cost Ratio (B/C)} = \frac{B}{C} \tag{7-4}$$

where higher-valued ratios indicate better risk mitigation actions from a cost-effectiveness standpoint. The probability that a target benefit-to-cost ratio, α, will be realized can be determined as (Ayyub 2003)

$$\Pr\left(\frac{B}{C} \geq \alpha\right) = 1 - \Pr(B - \alpha C \leq 0) \tag{7-5}$$

In addition to the results of Eq. 7-9, selection of a suitable risk mitigation action must also consider the affordability of each alternative and whether it achieves risk reduction objectives (McGill et al. 2007).

Conclusions

Quantifying risk using a probabilistic framework produces hazard (elevation) and loss-exceedance rates based on a spectrum of hurricanes according the joint probability distribution of the characteristic parameters that define hurricane intensity and the resulting surges, waves, and precipitation. The methodology provides a process for evaluating the performance of a hurricane protection system consisting of levees, floodwalls, transitions, closure gates, drainage systems and pumping stations, and measures population and property at risk by considering the stage-storage relationships of subbasins. The quantification of risk will enable decision-makers to consider various alternatives to manage risk through the enhancement of the hurricane protection systems, controlling land use, improving evacuation effectiveness, and improving system operations.

Acknowledgments

The author acknowledges the assistance of William McGill; and the discussions, input, and comments provided by Jerry Foster, Ed Link, Bruce Muller, Donald R. Dressler, Anjana Chudgar, John J. Jaeger, Gregory Baecher, Brian Blanton, David Bowles, Jennifer Chowning, Robert Dean, David Divoky, Bruce Ellingwood, Richalie Griffith, Harvey W. Jones, Mark Kaminskiy, Burton Kemp, Fred Krimgold, Therese McAllister, Martin W. McCann, Robert Patev, David Schaaf, Terry Sullivan, Pat Taylor, Nancy Towne, Daniele Veneziano, Gregory Walker, Mathew Watts, Allyson Windham, and Andy Harkness.

References

Ayyub, B. M. 2003. Risk Analysis in Engineering and Economics, Chapman & Hall/CRC Press, FL.

Daugherty, R., Franzini, J., and Finnemore E., 1985, Fluid Mechanics with Engineering Applications, 598 p., McGraw-Hill Book Co., NY.

Kumamoto, H., and Henley, E.J., 1996, Probabilistic Risk Assessment and Management for Engineers and Scientists, Second Edition, IEEE Press, New York.

McGill, W. L., Ayyub, B. M., and Kaminskiy, M. (2007). “Risk Analysis for Critical Asset Protection.” Risk Analysis. In press.

Modarres, M., Kaminskiy, M., and Krivstov, V., 1999. Reliability Engineering and Risk Analysis: A Practical Guide, Marcel Decker Inc., New York, NY.

USACE, 2006. Interagency Performance Evaluation Task Force Draft Report on “Performance Evaluation of the New Orleans and Southeast Louisiana Hurricane Protection System,” Draft Volume VIII – Engineering and Operational Risk and Reliability Analysis, USACE, Washington, DC. https://IPET.wes.army.mil.

This page intentionally left blank

Index